

# Temporally Smoothed Incremental Heuristic Dynamic Programming for Command-filtered Cascaded Online Learning Flight Control System

Yifei Li, Erik-Jan van Kampen

## Abstract

Online reinforcement learning has demonstrated the ability to adjust control laws using data-driven policy gradients. Its application to online learning flight control commonly employs a cascaded control architecture, which enables efficient policy learning for angle-of-attack tracking via control-surface deflections. However, tracking performance and system stability are often degraded by oscillatory actions. To address this issue, we incorporate temporal action smoothness into the Incremental Heuristic Dynamic Programming (IHDP) framework and employ a low-pass filter to attenuate oscillatory control commands. The Fast Fourier Transform (FFT) is used to analyze action smoothness in the frequency domain. Flight control simulations demonstrate the effectiveness of the proposed techniques.

## Index Terms

reinforcement learning, symmetry, data augmentation, approximate value iteration, flight control.

## I. INTRODUCTION

Online reinforcement learning (RL) has been applied to flight control law optimization without using an accurate system model for state prediction [1]–[15]. This approach significantly reduce the effort required to model the complex dynamics of aerial vehicles in control design, as the policy gradient is constructed using measured data. Online RL implemented within the model-based ADP framework typically relies on an accurate system model [16], or an approximator, such as an artificial neural network (ANN), to learn the system dynamics for state prediction [17]. In contrast, online learning implemented within model-free RL does not require learning a full system model, since only the first-order derivatives of the system dynamics are needed to construct the policy gradients [11], [15]. This motivates the use of a simpler model with fewer parameters than a nonlinear approximator, while still capturing the first-order derivatives, such as an *incremental model*, thereby simplifying the training process. The incremental model is a local linear approximation of a nonlinear system derived using Taylor expansion [18]. The combination with Recursive Least Squares (RLS) identification in ADP framework has led to the development of incremental model-based ADP methods, enabling computationally efficient online policy learning [11], [15]. Compared with action dependent heuristic dynamic programming (ADHDP), which implicitly approximates the control effectiveness within a state-action value ( $Q$ ) function [19], [20], the RLS algorithm quickly and accurately identifies the local control effectiveness represented in an incremental model, leading to a more reliable construction of the policy gradient, as demonstrated in simple cases [Ref (IHDP versus ADHDP)]. For example, incremental model-based heuristic dynamic programming (IHDP) requires only the signs of the control effectiveness matrix  $G$  to characterize the gradient directions [11], thereby using less model information than other IADP variants, such as incremental model-based dual heuristic programming (IDHP) [3] and incremental model-based global dual heuristic programming (IGDHP) [7]–[10].

The theoretical analysis of online ADHDP has been studied in [19], [20], where gradient descent algorithm is used to update both the critic and the actor. The ultimate uniform boundedness (UUB) of the network weights with respect to suboptimal values is established. As not using a state-action value ( $Q$ ) function, IHDP updates the critic in the same manner as ADHDP, but updates the actor using an estimated value function reconstructed according to the Bellman equation. This approach requires the signs of control effectiveness to construct the policy gradient. Also, it renders the backward construction of the Bellman error infeasible. These differences necessitate a formulation of the convergence analysis of IHDP, which has not been previously studied.

IHDP has been applied to online learning-based angle-of-attack (AOA) tracking control for a generic aerial vehicle model [11], [15]. A cascaded control structure is commonly employed, in which angle-of-attack tracking is regulated in the outer loop and pitch-rate tracking in the inner loop, enabling a *hierarchical* control strategy. The primary benefit of this structure lies in the explicit incorporation of pitch-rate constraints. By comparison, a monolithic structure can constrain the pitch rate through penalization in the reward design; however, the pitch-rate reference is not explicitly learned, which leads to degraded rate-control

Yifei Li was with the Section Control and Simulation, Faculty of Aerospace Engineering, Delft University of Technology, Delft, 2629 HS, the Netherlands, e-mail: y.li-34@tudelft.nl.

Erik-Jan van Kampen was with the Section Control and Simulation, Faculty of Aerospace Engineering, Delft University of Technology, Delft, 2629 HS, the Netherlands, e-mail: e.vankampen@tudelft.nl.

Manuscript received Month Day, Year; revised Month Day, Year.

performance. In addition, rate-control performance is sensitive to the weighting of the pitch-rate loss term. In backstepping, a stabilizing pitch-rate reference policy is derived from a nominal model, ensuring convergence of the tracking errors, with adaptive laws employed to handle model uncertainties [21], [22]. However, data-driven pitch-rate reference optimization in the model-free IHDP framework does not guarantee a consistently stabilizing policy during learning.

In nonlinear time-varying (NLTV) tracking error dynamics, time-varying nonlinearities and angle-of-attack reference signals induce frequent switching of the tracking error near zero. Consequently, the actor produces rapidly switching control actions, leading to system oscillations. This behavior is more severe than that observed in stabilizing linear time-invariant (LTI) systems.

A third factor contributing to oscillations in flight control systems is actor saturation, whereby the actor outputs maximum or minimum control actions in response to tracking errors that switch near zero, a behavior commonly referred to as *bang-bang control* [23]. In this regime, the saturated actor yields vanishing policy gradients due to the activation functions, causing the network weights to become nearly fixed and difficult to adapt. To mitigate this issue, discounted learning rates have been employed to slow actor updates over time, thereby reducing the likelihood of entering the saturation region [3], [8]. However, this approach has several limitations: the learning rate schedule is selected empirically and is sensitive to tuning, and it does not completely prevent actor saturation as learning progresses. Another potential solution is to terminate actor updates by fixing the network weights once the desired control performance is achieved, for example by specifying a termination time or a tracking-error threshold; however, this strategy has not yet been systematically studied.

In summary, these practical challenges degrade tracking control performance in cascaded online learning flight control systems and highlight the critical importance of ensuring action smoothness during learning.

Action smoothness in offline learning has been investigated through Conditioning for Action Policy Smoothness (CAPS) at both temporal and spatial scales [24]. Temporal smoothness loss significantly reduces the amplitude of switching motor actions in quadrotor control. Subsequent applications include flight control of the Flying-V and the Cessna Citation aircraft [25]–[28]. In online learning, the limited number of samples renders the computation of a spatial smoothness loss impractical, as it requires generating spatially biased state samples from a prior state distribution. Therefore, we focus exclusively on temporally smoothed flight control in online learning.

The low-pass filter effectively removes noise and fast-switching signals in flight control systems, such as command-filtered backstepping [21], [22]. By tuning the natural frequency, it smooths control commands from a frequency-domain perspective, even for small-amplitude signals. This complements the temporal smoothness loss, which is less effective at attenuating commands with small amplitudes.

The main contributions are summarized as follows.

- We develop temporally smoothed incremental heuristic dynamic programming (TS-IHDP), to learn an action-increment constrained policy. The UUB convergence of the estimated weights of the critic and actor to suboptimal values is proved via trace analysis. The incorporation of a temporal loss brings new convergence results.
- The cascaded online learning flight control simulations demonstrate that TS-IHDP and command-filtered TS-IHDP generate smooth pitch rate references and control surface deflections, reducing system oscillations and improving the system stability.
- Termination and restart conditions are designed to adaptively control the online learning process based on tracking errors over sliding past-time windows.

The remainder of this paper is structured as follows. Section II introduces the incremental model and recursive least square identification. Section III formulates the TS-IHDP method, with weight updated using gradient descent. The convergence of network weights is proved in Section IV. Section V designs a cascaded online learning flight control system. Section VI presents simulation results. Section VII concludes this paper.

## II. PRELIMINARIES

### A. Incremental Model

Consider a continuous nonlinear system

$$\dot{x}(t) = f(x(t), u(t)) \quad (1)$$

where the dynamics  $f : \mathbb{R}^n \times \mathbb{R}^m \rightarrow \mathbb{R}^n$  is a smooth function associated with state vector  $x \in \mathbb{R}^n$  and input vector  $u \in \mathbb{R}^m$ ,  $n, m$  are positive integers denoting the dimensions of the state and action spaces.

Taking Taylor expansion at  $t_0$ :

$$\begin{aligned} f(x(t), u(t)) = & f(x(t_0), u(t_0)) + F(t_0)(x(t) - x(t_0)) + G(t_0)(u(t) - u(t_0)) \\ & + O[(x(t) - x(t_0))^2, (u(t) - u(t_0))^2] \end{aligned} \quad (2)$$

where  $F(t_0) = \partial f(x, u)/\partial x|_{x(t_0), u(t_0)} \in \mathbb{R}^{n \times n}$ ,  $G(t_0) = \partial f(x, u)/\partial u|_{x(t_0), u(t_0)} \in \mathbb{R}^{n \times m}$  are first-order partial derivatives.  $O(\cdot)$  is the summed higher-order terms.

As the term  $O(\cdot)$  has a relatively small influence on the state transition from  $x_t$  to  $x_{t+1}$  compared with the first-order terms, and because the higher-order derivatives of  $f(x(t), u(t))$  are difficult to identify from data, incorporating these higher-order terms into the model is impractical. Therefore, we omit  $O(\cdot)$  to define an effective and practical model for the nonlinear system:

$$f(x(t), u(t)) = f(x(t_0), u(t_0)) + F(t_0)(x(t) - x(t_0)) + G(t_0)(u(t) - u(t_0)) \quad (3)$$

Use Equation 1:

$$\dot{x}(t) = \dot{x}(t_0) + F(t_0)[x(t) - x(t_0)] + G(t_0)[u(t) - u(t_0)] \quad (4)$$

Use the approximation for derivatives  $\dot{x}(t) \approx \frac{x(t+T) - x(t)}{T}$  and  $\dot{x}(t_0) \approx \frac{x(t_0+T) - x(t_0)}{T}$ , where  $T$  is a constant time step. Then

$$\frac{x(t+T) - x(t)}{T} \approx \frac{x(t_0+T) - x(t_0)}{T} + F(t_0)[x(t) - x(t_0)] + G(t_0)[u(t) - u(t_0)] \quad (5)$$

Define a discretization approach over  $T$  by setting  $t_0 = (k-1)T$ ,  $x(t_0) = x((k-1)T) \triangleq x_{k-1}$ . Let  $x(t)$  denote the next-step state following  $x(t_0)$ , then  $x(t) = x(t_0 + T) \triangleq x_k$ .

A discretized version of system 5 is

$$x_{k+1} - x_k \approx x_k - x_{k-1} + F_{k-1}(x_k - x_{k-1})T + G_{k-1}(u_k - u_{k-1})T \quad (6)$$

Use denotations  $\Delta x(k+1) = x(k+1) - x(k)$ ,  $\Delta x(k) = x(k) - x(k-1)$ ,  $\Delta u(k) = x(k) - x(k-1)$ :

$$\Delta x_{k+1} = \Delta x_k + T F_{k-1} \Delta x_k + T G_{k-1} \Delta u_k \quad (7)$$

### B. Recursive Least Squares identification

The Recursive Least Squares (RLS) algorithm identifies  $F_{k-1}, G_{k-1}$  in the incremental model online [29]. Define the augmented state as  $\mathbf{x}_k = [\Delta x_k, \Delta u_k]^T$  and estimated parameter as  $\hat{\theta}_{k-1} = [\hat{F}_{k-1}, \hat{G}_{k-1}]^T$ . The one-step state prediction is  $\hat{\mathbf{x}}_{k+1}^T = \mathbf{x}_k^T \hat{\theta}_{k-1}$ . The error between the true state and predicted state is  $\varepsilon_k = \Delta \mathbf{x}_{k+1}^T - \hat{\mathbf{x}}_{k+1}^T$ . The estimated parameter is updated by

$$\hat{\theta}_k = \hat{\theta}_{k-1} + P_k \mathbf{x}_k \varepsilon_k \quad (8)$$

$$\begin{aligned} P_k^{-1} &= \alpha P_{k-1}^{-1} + \mathbf{x}_k \mathbf{x}_k^T \\ &= \sum_{j=1}^k \alpha^{k-j} \mathbf{x}_j \mathbf{x}_j^T + \alpha^k P_0^{-1} \\ &= \sum_{j=1}^k \alpha^{k-j} \mathbf{x}_j \mathbf{x}_j^T + I \alpha^k \lambda_{\min}(0) \end{aligned} \quad (9)$$

The initial auxiliary matrix is set as  $P_0 = I / \lambda_{\min}(0)$ , where  $0 < \lambda_{\min}(0) \ll 1$  is the minimum eigenvalue of  $P_0^{-1}$ . The initial parameter matrix is  $\hat{\theta}_0$ . The forgetting factor is  $0 \ll \alpha < 1$ .

## III. TEMPORALLY SMOOTHED INCREMENTAL MODEL-BASED HEURISTIC DYNAMIC PROGRAMMING

### A. Problem formulation

Consider a nonlinear dynamical system model as

$$x(t+1) = f(x(t), u(t)) \quad (10)$$

The cost-to-go function is expressed as

$$V(x(t)) = \sum_{i=t}^{\infty} \alpha^{i-t} c(x(i), u(i)), \quad (11)$$

where  $\alpha \in (0, 1]$  is the discount factor,  $c(x(t), u(t)) = x^T(t)Qx(t) + u^T(t)Ru(t)$  is the one-step cost function. We require  $c(t) = c(x(t), u(t))$  to be a bounded semidefinite function of the state and control. One can obtain from (11) that  $0 = V(t) - c(t) - \alpha V(t+1)$ , where  $V(t) = V(x(t))$ .

### B. Critic network

The critic is a one-hidden-layer multilayer perceptron (MLP) that takes the input as  $y(t) = (x_1(t), \dots, x_m(t))^T$  and the output as approximated cost-to-go function  $\hat{V}(t)$ . The number of nodes in hidden layer is  $N_{h_c}$ . The weight between input node  $i$  and hidden node  $j$  is  $\hat{w}_{c,ji}^{(1)}(t)$ . The weight between hidden node  $j$  and output node is  $\hat{w}_{c,j}^{(2)}(t)$ .

The input to hidden node  $j$  is:

$$\sigma_{c,j}(t) = \sum_{i=1}^m \hat{w}_{c,ji}^{(1)}(t) x_i(t) \quad (12)$$

The output of hidden node  $j$  is

$$\phi_{c,j}(t) = \tanh(\sigma_{c,j}(t)) \quad (13)$$

where  $\tanh(\cdot)$  is the nonlinear activation function.

The output of the critic is

$$\hat{V}(t) = \sum_{j=1}^{N_{h_c}} \hat{w}_{c,j}^{(2)}(t) \phi_{c,j}(t), \quad (14)$$

### C. Actor network

The actor is a one-hidden-layer multilayer perceptron (MLP) that takes the input as the state  $x(t) = (x_1(t), \dots, x_m(t))^T$ , and the output as the action  $[u_1(t), \dots, u_n(t)]^T$ . The number of nodes in hidden layer is  $N_{h_a}$ . The weight between input node  $i$  and hidden node  $j$  is  $\hat{w}_{a,ji}^{(1)}(t)$ . The weight between hidden node  $j$  and output node  $k$  is  $\hat{w}_{a,kj}^{(2)}(t)$ .

The input to hidden node  $j$  is

$$\sigma_{a,j}(t) = \sum_{i=1}^m \hat{w}_{a,ji}^{(1)}(t) x_i(t). \quad (15)$$

The output of hidden node  $j$  is:

$$\phi_{a,j}(t) = \tanh(\sigma_{a,j}(t)) \quad (16)$$

The hidden to output node is

$$\sigma_{a,k}(t) = \sum_{j=1}^{N_{h_a}} \hat{w}_{a,kj}^{(2)}(t) \phi_{a,j}(t) \quad (17)$$

The output of the output node  $k$  is

$$u_k(t) = \tanh(\sigma_{a,k}(t)) \quad (18)$$

### D. Update of the critic network

The critic network is trained to minimize the objective function  $E_c(t) = \frac{1}{2} e_c^2(t)$ , where  $e_c(t) = \hat{V}(t) - c(t) - \alpha \hat{V}(t+1)$  is the Bellman error. In ADHDP [19], [20], the definition of  $e_c(t)$  adopts a backward formulation to facilitate policy improvement based on the state-action value function. In contrast, this work employs a forward formulation, since policy evaluation in IHDP requires one-step-ahead state samples.

The weights between the input layer and the hidden layer are updated as

$$\hat{w}_c^{(1)}(t+1) = \hat{w}_c^{(1)}(t) + \Delta \hat{w}_c^{(1)}(t) \quad (19)$$

where  $\hat{w}_c^{(1)} \in \mathbb{R}^{N_{h_c} \times m}$ .

Using gradient descent, the element-wise weight update is given by

$$\Delta \hat{w}_{c,ji}^{(1)}(t) = l_c \left[ -\frac{\partial E_c(t)}{\partial \hat{w}_{c,ji}^{(1)}(t)} \right] \quad (20)$$

which follows directly from the chain rule

$$\begin{aligned} \frac{\partial E_c(t)}{\partial \hat{w}_{c,ji}^{(1)}(t)} &= \frac{\partial E_c(t)}{\partial e_c(t)} \frac{\partial e_c(t)}{\partial \hat{V}(t)} \frac{\partial \hat{V}(t)}{\partial \phi_{c,j}(t)} \frac{\partial \phi_{c,j}(t)}{\partial \sigma_{c,j}(t)} \frac{\partial \sigma_{c,j}(t)}{\partial \hat{w}_{c,ji}^{(1)}(t)} \\ &= e_c(t) \hat{w}_{c,j}^{(2)}(t) \phi'_{c,j}(t) y_i(t) \end{aligned} \quad (21)$$

The weights between the hidden layer and the output layer are updated as

$$\hat{w}_c^{(2)}(t+1) = \hat{w}_c^{(2)}(t) + \Delta \hat{w}_c^{(2)}(t) \quad (22)$$

where  $\hat{w}_c^{(2)} \in \mathbb{R}^{1 \times N_{h_c}}$ .

Using gradient descent, the element-wise weight update is given by

$$\Delta \hat{w}_{c,j}^{(2)}(t) = l_c \left[ -\frac{\partial E_c(t)}{\partial \hat{w}_{c,j}^{(2)}(t)} \right] \quad (23)$$

which follows directly from the chain rule

$$\frac{\partial E_c(t)}{\partial \hat{w}_{c,j}^{(2)}(t)} = \frac{\partial E_c(t)}{\partial e_c(t)} \frac{\partial e_c(t)}{\partial \hat{V}(t)} \frac{\partial \hat{V}(t)}{\partial \hat{w}_{c,j}^{(2)}(t)} = e_c(t) \phi_{c,j}(t) \quad (24)$$

#### E. Update of the actor network

The actor network is trained according to a value-based target constructed from the Bellman equation as  $P(t) = c(t) + \alpha \hat{V}(t+1)$ , rather than a state-action value function  $\hat{Q}(x(t), u(t))$  as in ADHDP [19], [20]. Let  $U_c$  denote the desired ultimate objective function. The quadratic error measure to be minimized is  $E_a(t) = E_{a1}(t) + \lambda E_{a2}(t)$ ,  $E_{a1}(t) = \frac{1}{2} e_a^2(t)$ ,  $E_{a2}(t) = \frac{1}{2} e_s^2(t)$ ,  $e_a(t) = c(t) + \alpha \hat{V}(t+1) - U_c$ ,  $e_s(t) = \frac{1}{2} \|u(t) - u(t+1)\|^2$ .  $\|\cdot\|$  is the Euclidean norm.  $e_s(t)$  is a temporal smoothness measure weighted by  $\lambda \geq 0$ . In reinforcement learning, success corresponds to an objective that is zero at each time step. For mathematical convenience, we assume  $U_c = 0$ , i.e.  $e_a(t) = c(t) + \alpha \hat{V}(t+1)$ .

The weights between the input layer and the hidden layer are updated as

$$\hat{w}_a^{(1)}(t+1) = \hat{w}_a^{(1)}(t) + \Delta \hat{w}_a^{(1)}(t) \quad (25)$$

where  $\hat{w}_a^{(1)} \in \mathbb{R}^{N_{h_c} \times m}$ , and the element-wise weight increment is given by

$$\Delta \hat{w}_{a,ji}^{(1)}(t) = l_a \left[ -\frac{\partial E_{a1}(t)}{\partial \hat{w}_{a,ji}^{(1)}(t)} - \lambda \frac{\partial E_{a2}(t)}{\partial \hat{w}_{a,ji}^{(1)}(t)} \right], \quad (26)$$

Applying the chain rule:

$$\begin{aligned} \frac{\partial E_{a1}(t)}{\partial \hat{w}_{a,ji}^{(1)}(t)} &= \frac{\partial E_{a1}(t)}{\partial e_a(t)} \left[ \frac{\partial e_a(t)}{\partial u(t)} \right]^T \frac{\partial u(t)}{\partial \sigma_{a,j}(t)} \frac{\partial \sigma_{a,j}(t)}{\partial \hat{w}_{a,ji}^{(1)}(t)} \\ &= \frac{\partial E_{a1}(t)}{\partial e_a(t)} \sum_{k=1}^n \frac{\partial e_a(t)}{\partial u_k(t)} \frac{\partial u_k(t)}{\partial \sigma_{a,k}(t)} \frac{\partial \sigma_{a,k}(t)}{\partial \phi_{a,j}(t)} \frac{\partial \phi_{a,j}(t)}{\partial \sigma_{a,j}(t)} \frac{\partial \sigma_{a,j}(t)}{\partial \hat{w}_{a,ji}^{(1)}(t)} \\ &= \frac{\partial E_{a1}(t)}{\partial e_a(t)} \sum_{k=1}^n \left( \frac{\partial c(t)}{\partial u(t)} + \alpha \left[ \frac{\partial \hat{V}(t+1)}{\partial x(t+1)} \right]^T \frac{\partial x(t+1)}{\partial u(t)} \right)_k \frac{\partial u_k(t)}{\partial \sigma_{a,k}(t)} \frac{\partial \sigma_{a,k}(t)}{\partial \phi_{a,j}(t)} \frac{\partial \phi_{a,j}(t)}{\partial \sigma_{a,j}(t)} \frac{\partial \sigma_{a,j}(t)}{\partial \hat{w}_{a,ji}^{(1)}(t)} \quad (27) \\ &= \frac{\partial E_{a1}(t)}{\partial e_a(t)} \sum_{k=1}^n \left( 2R u(t) + \alpha \left[ \frac{\partial \hat{V}(t+1)}{\partial x(t+1)} \right]^T G(t-1) \right)_k \frac{\partial u_k(t)}{\partial \sigma_{a,k}(t)} \frac{\partial \sigma_{a,k}(t)}{\partial \phi_{a,j}(t)} \frac{\partial \phi_{a,j}(t)}{\partial \sigma_{a,j}(t)} \frac{\partial \sigma_{a,j}(t)}{\partial \hat{w}_{a,ji}^{(1)}(t)} \\ &= e_a(t) \sum_{k=1}^n \left( 2R u(t) + \left[ \alpha \hat{w}_c^{(2)}(t) \phi'(x(t+1)) \hat{w}_c^{(1)}(t) \right]^T G(t-1) \right)_k \phi'_{a,k}(t) \hat{w}_{a,kj}^{(2)}(t) \phi'_{a,j}(t) x_i(t) \end{aligned}$$

and

$$\begin{aligned} \frac{\partial E_{a2}(t)}{\partial \hat{w}_{a,ji}^{(1)}(t)} &= \frac{\partial E_{a2}(t)}{\partial e_s(t)} \left[ \frac{\partial e_s(t)}{\partial u(t)} \right]^T \frac{\partial u(t)}{\partial \sigma_{a,k}(t)} \frac{\partial \sigma_{a,k}(t)}{\partial \phi_{a,j}(t)} \frac{\partial \phi_{a,j}(t)}{\partial \sigma_{a,j}(t)} \frac{\partial \sigma_{a,j}(t)}{\partial \hat{w}_{a,ji}^{(1)}(t)} \\ &= \frac{\partial E_{a2}(t)}{\partial e_s(t)} \sum_{k=1}^n \frac{\partial e_s(t)}{\partial u_k(t)} \frac{\partial u_k(t)}{\partial \sigma_{a,k}(t)} \frac{\partial \sigma_{a,k}(t)}{\partial \phi_{a,j}(t)} \frac{\partial \phi_{a,j}(t)}{\partial \sigma_{a,j}(t)} \frac{\partial \sigma_{a,j}(t)}{\partial \hat{w}_{a,ji}^{(1)}(t)} \quad (28) \\ &= e_s(t) \sum_{k=1}^n (u_k(t) - u_k(t+1)) \phi'_{a,k}(t) \hat{w}_{a,kj}^{(2)}(t) \phi'_{a,j}(t) x_i(t) \end{aligned}$$

The weights between the hidden layer and the output layer are updated as

$$\hat{w}_a^{(2)}(t+1) = \hat{w}_a^{(2)}(t) + \Delta \hat{w}_a^{(2)}(t) \quad (29)$$

where  $\hat{w}_a^{(2)} \in \mathbb{R}^{n \times N_{h_a}}$ , and the element-wise weight increment is

$$\Delta \hat{w}_{a,kj}^{(2)}(t) = l_a \left[ -\frac{\partial E_{a1}(t)}{\partial \hat{w}_{a,kj}^{(2)}(t)} - \lambda \frac{\partial E_{a2}(t)}{\partial \hat{w}_{a,kj}^{(2)}(t)} \right] \quad (30)$$

Applying the chain rule:

$$\begin{aligned} \frac{\partial E_{a1}(t)}{\partial \hat{w}_{a,kj}^{(2)}(t)} &= \frac{\partial E_{a1}(t)}{\partial e_a(t)} \frac{\partial e_a(t)}{\partial u_k(t)} \frac{\partial u_k(t)}{\partial \sigma_{a,k}(t)} \frac{\partial \sigma_{a,k}(t)}{\partial \hat{w}_{a,kj}^{(2)}(t)} \\ &= \frac{\partial E_{a1}(t)}{\partial e_a(t)} \left( \frac{\partial c(t)}{\partial u(t)} + \alpha \left[ \frac{\partial \hat{V}(t+1)}{\partial x(t+1)} \right]^T \frac{\partial x(t+1)}{\partial u(t)} \right)_k \frac{\partial u_k(t)}{\partial \sigma_{a,k}(t)} \frac{\partial \sigma_{a,k}(t)}{\partial \hat{w}_{a,kj}^{(2)}(t)} \\ &= e_a(t) \left( 2R u(t) + \alpha \left[ \frac{\partial \hat{V}(t+1)}{\partial x(t+1)} \right]^T G(t-1) \right)_k \phi'_{a,k}(t) \phi_{a,j}(t) \\ &= e_a(t) \left( 2R u(t) + \alpha \left[ \hat{w}_c^{(2)}(t) \phi'(x(t+1)) \hat{w}_c^{(1)}(t) \right]^T G(t-1) \right)_k \phi'_{a,k}(t) \phi_{a,j}(t) \end{aligned} \quad (31)$$

and

$$\begin{aligned} \frac{\partial E_{a2}(t)}{\partial \hat{w}_{a,kj}^{(2)}(t)} &= \frac{\partial E_{a2}(t)}{\partial e_s(t)} \frac{\partial e_s(t)}{\partial u_k(t)} \frac{\partial u_k(t)}{\partial \sigma_{a,k}(t)} \frac{\partial \sigma_{a,k}(t)}{\partial \hat{w}_{a,kj}^{(2)}(t)} \\ &= e_s(t) (u_k(t) - u_k(t+1)) \phi'_{a,k}(t) \phi_{a,j}(t) \end{aligned} \quad (32)$$

**Remark 1.** The temporal action smoothness loss  $E_{a2}(t)$  enables learning an action-increment-constrained policy, which is absent in standard IHDP and ADHDP formulations.

#### IV. CONVERGENCE ANALYSIS

##### A. Basics of uniformly ultimately bounded stability

Denote the ideal (suboptimal) weights by  $w_c^*, w_a^*$ , defined as  $w_c^* = \arg \min_{\hat{w}_c} \left\| \hat{V}(t) - c(t) - \alpha \hat{V}(t+1) \right\|^2$ , and  $w_a^* = \arg \min_{\hat{w}_a} \left( \|c(t) + \alpha \hat{V}(t+1)\|^2 + \frac{1}{2} \lambda \|u(t) - u(t+1)\|^2 \right)$  if assuming  $U_c = 0$ . The estimation errors of the critic and actor weights are defined by  $\tilde{w}(t) := \hat{w}(t) - w^*$ . Then, Equations (21),(24),(27),(28),(31),(32) define a dynamical system of estimation errors for a nonlinear function  $F$ :

$$\tilde{w}(t+1) = \tilde{w}(t) - F(\hat{w}(t), x(t), x(t+1)) \quad (33)$$

**Definition 1.** A dynamical system is said to be uniformly ultimately bounded (UUB) with ultimate bound  $\varepsilon > 0$ , if for any  $\delta > 0$  and  $t_0 > 0$ , there exists a positive number  $N = N(\delta, \varepsilon)$  independent of  $t_0$ , such that  $\|\tilde{w}(t)\| \leq \varepsilon$ , for all  $t \geq N + t_0$ , whenever  $\|\tilde{w}(t_0)\| \leq \delta$ .

**Theorem 1** (UUB of a discrete dynamical system). If, for system (33), there exists a function  $L(\tilde{w}(t), t)$  such that for all  $\tilde{w}(t_0)$  in a compact set  $K$ ,  $L(\tilde{w}(t), t)$  is positive definite and the first difference satisfies  $\Delta L(\tilde{w}(t), t) < 0$ , for  $\|\tilde{w}(t_0)\| > \varepsilon$ , for some  $\varepsilon > 0$  such that the  $\varepsilon$ -neighborhood of  $\tilde{w}(t)$  is contained in  $K$ , then the system is UUB and the norm of the state is bounded within a neighborhood of  $\varepsilon$ .

### B. Network weights increments

The convergence of critic and actor weights is analyzed using gradient descent algorithm. The requirements on learning rate to stabilize the convergence are analyzed. The ultimate bound is also provided.

**Assumption 1.** The ideal (suboptimal) weights are bounded as  $\|w_c^*\| \leq w_c^{\max}$ ,  $\|w_a^*\| \leq w_a^{\max}$ .

**Lemma 1.** Under Assumption 1, define  $L_1(t) = \frac{1}{l_c} \text{tr} \left[ (\tilde{w}_c^{(2)}(t))^T \tilde{w}_c^{(2)}(t) \right]$ , and its first difference  $\Delta L_1(t) = L_1(t+1) - L_1(t)$  is

$$\Delta L_1(t) = l_c e_c^2(t) \|\phi_c(t)\|^2 + \|e_c(t) - \tilde{w}_c^{(2)}(t) \phi_c(t)\|^2 - \|\zeta_c(t)\|^2 - e_c^2(t) \quad (34)$$

where  $\zeta_c(t) = \tilde{w}_c^{(2)}(t) \phi_c(t)$  is the approximation error of the critic output.

*Proof.* According to (22), (23), (24) and the fact that  $w_c^{*(2)}$  is time-invariant:

$$\tilde{w}_c^{(2)}(t+1) = \hat{w}_c^{(2)}(t+1) - w_c^{*(2)} = \tilde{w}_c^{(2)}(t) - l_c e_c(t) \phi_c^T(t) \quad (35)$$

where  $\phi_c(t) \in \mathbb{R}^{N_{h_c} \times 1}$ ,  $e_c(t)$  is a scalar.

The squared Frobenius norm of the critic weight error is given by

$$\begin{aligned} \text{tr} \left[ (\tilde{w}_c^{(2)}(t+1))^T \tilde{w}_c^{(2)}(t+1) \right] &= \text{tr} \left[ \left( \tilde{w}_c^{(2)}(t) - l_c e_c(t) \phi_c^T(t) \right)^T \left( \tilde{w}_c^{(2)}(t) - l_c e_c(t) \phi_c^T(t) \right) \right] \\ &= \text{tr} \left[ (\hat{w}_c^{(2)}(t))^T \tilde{w}_c^{(2)}(t) \right] + \text{tr} [l_c^2 e_c^2(t) \phi_c(t) \phi_c^T(t)] \\ &\quad - l_c e_c(t) \text{tr} \left[ (\tilde{w}_c^{(2)}(t))^T \phi_c^T(t) \right] - l_c e_c(t) \text{tr} \left[ \phi_c(t) \tilde{w}_c^{(2)}(t) \right] \\ &= \text{tr} \left[ (\hat{w}_c^{(2)}(t))^T \tilde{w}_c^{(2)}(t) \right] + \text{tr} [l_c^2 e_c^2(t) \phi_c(t) \phi_c^T(t)] \\ &\quad - 2 l_c e_c(t) \text{tr} \left[ \phi_c(t) \tilde{w}_c^{(2)}(t) \right] \\ &= \text{tr} \left[ (\hat{w}_c^{(2)}(t))^T \tilde{w}_c^{(2)}(t) \right] + l_c^2 e_c^2(t) \|\phi_c(t)\|^2 \\ &\quad - 2 l_c e_c(t) \tilde{w}_c^{(2)}(t) \phi_c(t) \end{aligned} \quad (36)$$

Since  $\tilde{w}_c^{(2)}(t) \phi_c(t)$  is a scalar, the cross term becomes

$$-2 l_c e_c(t) \tilde{w}_c^{(2)}(t) \phi_c(t) = l_c \left( \|e_c(t) - \tilde{w}_c^{(2)}(t) \phi_c(t)\|^2 - \|\tilde{w}_c^{(2)}(t) \phi_c(t)\|^2 - e_c^2(t) \right) \quad (37)$$

The difference  $\Delta L_1(t)$  yields

$$\begin{aligned} \Delta L_1(t) &= \frac{1}{l_c} \left( \text{tr}[(\tilde{w}_c^{(2)}(t+1))^T \tilde{w}_c^{(2)}(t+1)] - \text{tr}[(\tilde{w}_c^{(2)}(t))^T \tilde{w}_c^{(2)}(t)] \right) \\ &= l_c e_c^2(t) \|\phi_c(t)\|^2 + \|e_c(t) - \tilde{w}_c^{(2)}(t) \phi_c(t)\|^2 - \|\tilde{w}_c^{(2)}(t) \phi_c(t)\|^2 - e_c^2(t) \\ &= \underbrace{l_c e_c^2(t) \|\phi_c(t)\|^2 + \|e_c(t) - \tilde{w}_c^{(2)}(t) \phi_c(t)\|^2 - \|\zeta_c(t)\|^2 - e_c^2(t)}_{\Delta L_1(t)} \end{aligned} \quad (38)$$

where  $\zeta_c(t) = \tilde{w}_c^{(2)}(t) \phi_c(t)$ .  $\square$

**Lemma 2.** Under Assumption 1, define  $L_2(t) = \frac{1}{l_a \gamma_1} \text{tr} \left[ (\tilde{w}_a^{(2)}(t))^T \tilde{w}_a^{(2)}(t) \right]$ , and its first difference  $\Delta L_2(t) = L_2(t+1) - L_2(t)$  is bounded by

$$\begin{aligned} \Delta L_2(t) &= \frac{1}{l_a \gamma_1} \text{tr} \left( \tilde{w}_a^{(2)}(t+1)^T \tilde{w}_a^{(2)}(t+1) - \tilde{w}_a^{(2)}(t)^T \tilde{w}_a^{(2)}(t) \right) \\ &\leq \frac{1}{\gamma_1} \left( 2 l_a e_a^2(t) \|C(t)\|^2 \|\phi_a(t)\|^2 + 4 \|c(t)\|^2 + 8 \alpha^2 \|\zeta_a(t+1)\|^2 + 8 \alpha^2 \left\| w_a^{*(2)} \phi_a(t+1) \right\|^2 + \|C(t)\|^2 \|\zeta_a(t)\|^2 - e_a^2(t) \right) \\ &\quad + \frac{\lambda}{\gamma_1} \left( 2 \lambda l_a e_s^2(t) \|U(t)\|^2 \|\phi_a(t)\|^2 + 2 e_s^2(t) + \|U^T(t) \zeta_a(t)\|^2 - e_s^2(t) \right) \end{aligned} \quad (39)$$

where  $\zeta_a(t) = \tilde{w}_a^{(2)}(t)\phi_a(t)$ .

*Proof.* According to Equations (29)-(32) and the fact that  $w_a^{*(2)}$  is time-invariant:

$$\tilde{w}_a^{(2)}(t+1) = \hat{w}_a^{(2)}(t+1) - w_a^{*(2)} = \tilde{w}_a^{(2)}(t) - l_a e_a(t) C(t) \phi_a^T(t) - \lambda l_a e_s(t) U(t) \phi_a^T(t) \quad (40)$$

where  $\phi_a \in \mathbb{R}^{N_{ah} \times 1}$ ,  $C(t) \in \mathbb{R}^{n \times 1}$  and its element  $C_k(t) = \left(2Ru(t) + [\alpha \hat{w}_c^{(2)}(t)\phi'(x(t+1))\hat{w}_c^{(1)}(t)]^T G(t-1)\right)_k \phi'_{a,k}(t)$ ,  $U(t) \in \mathbb{R}^{n \times 1}$  and its element  $U_k(t) = (u_k(t) - u_k(t+1))\phi'_{a,k}(t)$ .

The squared Frobenius norm of the actor weight error is given by

$$\begin{aligned} & \text{tr} \left[ \left( \tilde{w}_a^{(2)}(t+1) \right)^T \tilde{w}_a^{(2)}(t+1) \right] \\ &= \text{tr} \left[ \left( \tilde{w}_a^{(2)}(t) - l_a e_a(t) C(t) \phi_a^T(t) - \lambda l_a e_s(t) U(t) \phi_a^T(t) \right)^T \left( \tilde{w}_a^{(2)}(t) - l_a e_a(t) C(t) \phi_a^T(t) - \lambda l_a e_s(t) U(t) \phi_a^T(t) \right) \right] \\ &= \text{tr} \left[ \left( \tilde{w}_a^{(2)}(t) \right)^T \tilde{w}_a^{(2)}(t) \right] + \text{tr} \left[ \left( l_a e_a(t) C(t) \phi_a^T(t) + \lambda l_a e_s(t) U(t) \phi_a^T(t) \right)^T \left( l_a e_a(t) C(t) \phi_a^T(t) + \lambda l_a e_s(t) U(t) \phi_a^T(t) \right) \right] \\ & \quad - l_a e_a(t) \text{tr} \left[ \left( \tilde{w}_a^{(2)}(t) \right)^T C(t) \phi_a^T(t) \right] - l_a e_a(t) \text{tr} \left[ \phi_a(t) C^T(t) \tilde{w}_a^{(2)}(t) \right] \\ & \quad - \lambda l_a e_s(t) \text{tr} \left[ \left( \tilde{w}_a^{(2)}(t) \right)^T U(t) \phi_a^T(t) \right] - \lambda l_a e_s(t) \text{tr} \left[ \phi_a(t) U^T(t) \tilde{w}_a^{(2)}(t) \right] \quad (41) \\ &= \text{tr} \left[ \left( \tilde{w}_a^{(2)}(t) \right)^T \tilde{w}_a^{(2)}(t) \right] + \text{tr} \left[ l_a^2 e_a^2(t) \phi_a(t) C^T(t) C(t) \phi_a^T(t) \right] + \text{tr} \left[ \lambda^2 l_a^2 e_s^2(t) \phi_a(t) U^T(t) U(t) \phi_a^T(t) \right] \\ & \quad + 2\lambda l_a^2 e_a(t) e_s(t) \text{tr} \left[ \phi_a(t) C^T(t) U(t) \phi_a^T(t) \right] - 2l_a e_a(t) \text{tr} \left[ \phi_a(t) C^T(t) \tilde{w}_a^{(2)}(t) \right] - 2\lambda l_a e_s(t) \text{tr} \left[ \phi_a(t) U^T(t) \tilde{w}_a^{(2)}(t) \right] \\ &= \text{tr} \left[ \left( \tilde{w}_a^{(2)}(t) \right)^T \tilde{w}_a^{(2)}(t) \right] + \underbrace{l_a^2 e_a^2(t) \|C(t)\|^2 \|\phi_a(t)\|^2}_{\text{term 1}} + \underbrace{\lambda^2 l_a^2 e_s^2(t) \|U(t)\|^2 \|\phi_a(t)\|^2}_{\text{term 2}} + \underbrace{-2l_a e_a(t) \text{tr} \left[ \phi_a(t) C^T(t) \tilde{w}_a^{(2)}(t) \right] - 2\lambda l_a e_s(t) \text{tr} \left[ \phi_a(t) U^T(t) \tilde{w}_a^{(2)}(t) \right]}_{\text{term 3}} \end{aligned}$$

Use  $\text{tr}(ABC) = \text{tr}(BCA)$  and Cauchy-Schwarz inequality in term 1:

$$\begin{aligned} \text{tr} \left[ \phi_a(t) C^T(t) U(t) \phi_a^T(t) \right] &= \text{tr} \left[ C^T(t) U(t) (\phi_a^T(t) \phi_a(t)) \right] \\ &= \text{tr} \left[ C^T(t) U(t) \right] \text{tr} [\phi^T(t) \phi(t)] \\ &\leq \|C(t)\| \|U(t)\| \|\phi(t)\|^2 \quad (42) \end{aligned}$$

Use  $2ab \leq a^2 + b^2$ :

$$\begin{aligned} 2\lambda l_a^2 e_a(t) e_s(t) \text{tr} \left[ \phi_a(t) C^T(t) U(t) \phi_a^T(t) \right] &\leq 2\lambda l_a^2 e_a(t) e_s(t) \|C(t)\| \|U(t)\| \|\phi(t)\|^2 \\ &\leq l_a^2 e_a^2(t) \|C(t)\|^2 \|\phi(t)\|^2 + \lambda^2 l_a^2 e_s^2(t) \|U(t)\|^2 \|\phi(t)\|^2 \quad (43) \end{aligned}$$

Consider the cross term 2, and use  $\text{tr}(ABC) = \text{tr}(BCA)$ :

$$\begin{aligned} -2l_a e_a(t) \text{tr} \left( \phi_a(t) C^T(t) \tilde{w}_a^{(2)}(t) \right) &= -2l_a e_a(t) \text{tr} \left( C^T(t) \tilde{w}_a^{(2)}(t) \phi_a(t) \right) \\ &= -2l_a e_a(t) C^T(t) \tilde{w}_a^{(2)}(t) \phi_a(t) \\ &\leq l_a \left( \|e_a(t) - C^T(t) \tilde{w}_a^{(2)}(t) \phi_a(t)\|^2 - \|C^T(t) \tilde{w}_a^{(2)}(t) \phi_a(t)\|^2 - e_a^2(t) \right) \\ &\leq l_a \left( \|e_a(t) - C^T(t) \zeta_a(t)\|^2 - \|C^T(t) \zeta_a(t)\|^2 - e_a^2(t) \right) \quad (44) \end{aligned}$$

where  $\zeta_a(t) = \tilde{w}_a^{(2)}(t)\phi_a(t)$ .

Similarly,

$$\begin{aligned} -2\lambda l_a e_s(t) \text{tr} \left( \phi_a(t) U^T(t) \tilde{w}_a^{(2)}(t) \right) &= -2\lambda l_a e_s(t) \text{tr} \left( U^T(t) \tilde{w}_a^{(2)}(t) \phi_a(t) \right) \\ &= -2\lambda l_a e_s(t) U^T(t) \tilde{w}_a^{(2)}(t) \phi_a(t) \\ &\leq \lambda l_a \left( 2e_s^2(t) + \|U^T(t) \tilde{w}_a^{(2)}(t) \phi_a(t)\|^2 - e_s^2(t) \right) \quad (45) \end{aligned}$$

Notice that  $(a - b)^2 - b^2 \leq 2a^2 + b^2$ , and use  $\|C^T(t)\zeta_a(t)\|^2 \leq \|C^T(t)\|^2\|\zeta_a(t)\|^2$  by Cauchy–Schwarz inequality:

$$\begin{aligned}
& \|e_a(t) - C^T(t)\zeta_a(t)\|^2 - \|C^T(t)\zeta_a(t)\|^2 \\
& \leq 2\|e_a(t)\|^2 + \|C^T(t)\zeta_a(t)\|^2 \\
& \leq 2\left\|c(t) + \alpha\hat{V}(t+1)\right\|^2 + \|C^T(t)\zeta_a(t)\|^2 \\
& \leq 2\left(\|c(t)\| + \alpha\left\|\hat{V}(t+1)\right\|\right)^2 + \|C^T(t)\zeta_a(t)\|^2 \\
& \leq 4\|c(t)\|^2 + 4\alpha^2\left\|\hat{w}_c^{(2)}\phi_c(t+1)\right\|^2 + \|C^T(t)\zeta_a(t)\|^2 \\
& \leq 4\|c(t)\|^2 + 4\alpha^2\left\|(\tilde{w}_c^{(2)} + w_c^{*(2)})\phi_c(t+1)\right\|^2 + \|C^T(t)\zeta_a(t)\|^2 \\
& \leq 4\|c(t)\|^2 + 8\alpha^2\left\|\tilde{w}_c^{(2)}\phi_c(t+1)\right\|^2 + 8\alpha^2\left\|w_c^{*(2)}\phi_c(t+1)\right\|^2 + \|C^T(t)\zeta_a(t)\|^2 \\
& \leq 4\|c(t)\|^2 + 8\alpha^2\|\zeta_c(t+1)\|^2 + 8\alpha^2\left\|w_c^{*(2)}\phi_c(t+1)\right\|^2 + \|C^T(t)\zeta_a(t)\|^2 \\
& \leq 4\|c(t)\|^2 + 8\alpha^2\|\zeta_c(t+1)\|^2 + 8\alpha^2\left\|w_c^{*(2)}\phi_c(t+1)\right\|^2 + \|C(t)\|^2\|\zeta_a(t)\|^2
\end{aligned} \tag{46}$$

where  $\zeta_c(t+1) = \tilde{w}_c^{(2)}(t)\phi_c(t+1)$ .

Therefore, the first difference is

$$\begin{aligned}
\Delta L_2(t) &= \frac{1}{l_a\gamma_1}\text{tr}\left(\tilde{w}_a^{(2)}(t+1)^T\tilde{w}_a^{(2)}(t+1) - \tilde{w}_a^{(2)}(t)^T\tilde{w}_a^{(2)}(t)\right) \\
&\leq \frac{1}{\gamma_1}\left(2l_ae_a^2(t)\|C(t)\|^2\|\phi_a(t)\|^2 + 4\|c(t)\|^2 + 8\alpha^2\|\zeta_c(t+1)\|^2 + 8\alpha^2\left\|w_c^{*(2)}\phi_c(t+1)\right\|^2 + \|C(t)\|^2\|\zeta_a(t)\|^2 - e_a^2(t)\right) \\
&+ \frac{\lambda}{\gamma_1}\left(2\lambda l_ae_s^2(t)\|U(t)\|^2\|\phi_a(t)\|^2 + 2e_s^2(t) + \|U^T(t)\zeta_a(t)\|^2 - e_s^2(t)\right)
\end{aligned} \tag{47}$$

□

**Remark 2.** Note that  $\Delta L_2$  depends on  $C(t)$ , which incorporates the control-effectiveness matrix  $G_{t-1}$ . Thus, a system with high control effectiveness, i.e. a more “sensitive” system, may exhibit a larger bound. Intuitively, this matches our expectation.

**Remark 3.**  $C(t)$  is defined differently from [19] given the objective function to improve the policy, i.e.,  $r(t) + \hat{V}(t+1)$  in IHDP and  $\hat{V}(t)$  in ADHDP.

**Remark 4.** If we introduce the normalization  $\|(\hat{w}_c^{(2)}(t))^T C(t)\|^2 = 1$  and fix the input-layer weights, then Lemmas 1–2 yield the results of Liu et al. (2012).

**Lemma 3.** Under Assumption 1, define  $L_3(t) = \frac{1}{l_c\gamma_2}\text{tr}\left[(\tilde{w}_c^{(1)}(t))^T\tilde{w}_c^{(1)}(t)\right]$ , and its difference  $\Delta L_3(t) = L_3(t+1) - L_3(t)$  is bounded by

$$\Delta L_3(t) \leq \frac{1}{\gamma_2}\left(l_ce_c^2(t)\|a(t)\|^2\|y(t)\|^2 + \|a(t)\|^2\|\tilde{w}_c^{(1)}(t)y(t)\|^2 + e_c^2(t)\right) \tag{48}$$

where  $\gamma_2 > 0$  is a weighting factor and  $a(t) \in \mathbb{R}^{N_{h_c} \times 1}$  is a vector with  $a_j(t) = \hat{w}_{c,j}^{(2)}(t)\phi'_j(t)$ .

*Proof.* Consider the update rule (21), the weight error is

$$\tilde{w}_c^{(1)}(t+1) = \hat{w}_c^{(1)}(t+1) - w_c^{*(1)} = \tilde{w}_c^{(1)}(t) - l_ce_c(t)B(t) \tag{49}$$

where  $B(t) \in \mathbb{R}^{N_{h_c} \times m}$  and its element  $B_{ji}(t) = \hat{w}_{c,j}^{(2)}(t)\phi'_j(t)y_i(t)$ , then  $B(t) = a(t)y^T(t)$ .

The squared Frobenius norm of the actor weight error is given by

$$\begin{aligned}
\text{tr} \left[ \tilde{w}_c^{(1)}(t+1)^T \tilde{w}_c^{(1)}(t+1) \right] &= \text{tr} \left[ \left( \tilde{w}_c^{(1)}(t) - l_c e_c(t) B(t) \right)^T \left( \tilde{w}_c^{(1)}(t) - l_c e_c(t) B(t) \right) \right] \\
&= \text{tr} \left[ (\tilde{w}_c^{(1)}(t))^T \tilde{w}_c^{(1)}(t) \right] + \text{tr} \left[ l_c^2 e_c^2(t) B^T(t) B(t) \right] \\
&\quad - l_c e_c(t) \left[ (\tilde{w}_c^{(1)}(t))^T B(t) \right] - l_c e_c(t) \text{tr} \left[ B^T(t) \tilde{w}_c^{(1)}(t) \right] \\
&= \text{tr} \left[ (\tilde{w}_c^{(1)}(t))^T \tilde{w}_c^{(1)}(t) \right] + \text{tr} \left[ l_c^2 e_c^2(t) B^T(t) B(t) \right] \\
&\quad - 2 l_c e_c(t) \text{tr} \left[ B^T(t) \tilde{w}_c^{(1)}(t) \right] \\
&= \text{tr} \left[ (\tilde{w}_c^{(1)}(t))^T \tilde{w}_c^{(1)}(t) \right] + \text{tr} \left[ l_c^2 e_c^2(t) y(t) a^T(t) a(t) y^T(t) \right] \\
&\quad - 2 l_c e_c(t) \text{tr} \left[ B^T(t) \tilde{w}_c^{(1)}(t) \right] \\
&= \text{tr} \left[ (\tilde{w}_c^{(1)}(t))^T \tilde{w}_c^{(1)}(t) \right] + l_c^2 e_c^2(t) \|a(t)\|^2 \|y(t)\|^2 \\
&\quad - 2 l_c e_c(t) \text{tr} \left[ B^T(t) \tilde{w}_c^{(1)}(t) \right]
\end{aligned} \tag{50}$$

By  $\text{tr}(ABC) = \text{tr}(BCA)$ :

$$\begin{aligned}
\text{tr} \left[ B^T(t) \tilde{w}_c^{(1)}(t) \right] &= \text{tr} \left[ y(t) a^T(t) \tilde{w}_c^{(1)}(t) \right] \\
&= \text{tr} \left[ a^T(t) \tilde{w}_c^{(1)}(t) y(t) \right] \\
&= a^T(t) \tilde{w}_c^{(1)}(t) y(t)
\end{aligned} \tag{51}$$

Use inequality  $-2ab \leq a^2 + b^2$ , the cross term becomes

$$\begin{aligned}
-2 l_c e_c(t) a^T(t) \tilde{w}_c^{(1)}(t) y(t) &\leq l_c \left( \|a^T(t) \tilde{w}_c^{(1)}(t) y(t)\|^2 + e_c^2(t) \right) \\
&\leq l_c \left( \|a^T(t)\|^2 \|\tilde{w}_c^{(1)}(t) y(t)\|^2 + e_c^2(t) \right) \\
&\leq l_c \left( \|a(t)\|^2 \|\tilde{w}_c^{(1)}(t) y(t)\|^2 + e_c^2(t) \right)
\end{aligned} \tag{52}$$

Therefore, the first difference can be bounded by

$$\Delta L_3(t) \leq \underbrace{\frac{1}{\gamma_2} \left( l_c e_c^2(t) \|a(t)\|^2 \|y(t)\|^2 + \|a(t)\|^2 \|\tilde{w}_c^{(1)}(t) y(t)\|^2 + e_c^2(t) \right)}_{\Delta L_3(t)} \tag{53}$$

□

**Lemma 4.** Under Assumption 1, define  $L_4(t) = \frac{1}{l_a \gamma_3} \text{tr} \left[ \tilde{w}_a^{(1)}(t)^T \tilde{w}_a^{(1)}(t) \right]$ , and its first difference  $\Delta L_4(t) = L_4(t+1) - L_4(t)$  is bounded by

$$\Delta L_4(t) \leq \frac{1}{\gamma_3} \left( l_a e_a^2(t) \|C^T(t) D(t)\|^2 \|x(t)\|^2 + e_a^2(t) + \|C^T(t) D(t)\|^2 \left\| \tilde{w}_a^{(1)}(t) x(t) \right\|^2 \right) \tag{54}$$

where  $\gamma_3 > 0$  is a weighting factor, and  $D(t) \in \mathbb{R}^{n \times N_{h_a}}$ , and its element  $D_{kj}(t) = \hat{w}_{a,kj}^{(2)}(t) \phi'_{k,j}(x(t))$ .

*Proof.* According to Equations (25)-(28), the weight errors are

$$\begin{aligned}
\tilde{w}_a^{(1)}(t+1) &= \hat{w}_a^{(1)}(t+1) - w_a^{*(1)} \\
&= \tilde{w}_a^{(1)}(t) - l_a e_a(t) D^T(t) C(t) x^T(t) - \lambda l_a e_s(t) D^T(t) U(t) x^T(t)
\end{aligned} \tag{55}$$

and

$$\begin{aligned}
& \text{tr} \left[ \left( \tilde{w}_a^{(1)}(t+1) \right)^T \tilde{w}_a^{(1)}(t+1) \right] \\
&= \text{tr} \left[ \left( \tilde{w}_a^{(1)}(t) - l_a e_a(t) D^T(t) C(t) x^T(t) - \lambda l_a e_s(t) D^T(t) U(t) x^T(t) \right)^T \right. \\
&\quad \left. \left( \tilde{w}_a^{(1)}(t) - l_a e_a(t) D^T(t) C(t) x^T(t) - \lambda l_a e_s(t) D^T(t) U(t) x^T(t) \right) \right] \\
&= \text{tr} \left[ \left( \tilde{w}_a^{(1)}(t) \right)^T \tilde{w}_a^{(1)}(t) \right] + \text{tr} \left[ \left( l_a e_a(t) D^T(t) C(t) x^T(t) + \lambda l_a e_s(t) D^T(t) U(t) x^T(t) \right)^T \right. \\
&\quad \left. \left( l_a e_a(t) D^T(t) C(t) x^T(t) + \lambda l_a e_s(t) D^T(t) U(t) x^T(t) \right) \right] \\
&\quad - l_a \text{tr} \left[ \left( \tilde{w}_a^{(1)}(t) \right)^T \left( e_a(t) D^T(t) C(t) x^T(t) + \lambda e_s(t) D^T(t) U(t) x^T(t) \right) \right] \\
&\quad - l_a \text{tr} \left[ \left( e_a(t) x(t) C^T(t) D(t) + \lambda e_s(t) x(t) U^T(t) D(t) \right) \tilde{w}_a^{(1)}(t) \right] \\
&= \text{tr} \left[ \left( \tilde{w}_a^{(1)}(t) \right)^T \tilde{w}_a^{(1)}(t) \right] + l_a^2 e_a^2(t) \text{tr} \left[ x(t) C^T(t) D(t) D^T(t) C(t) x^T(t) \right] + \lambda^2 l_a^2 e_s^2(t) \text{tr} \left[ x(t) U^T(t) D(t) D^T(t) U(t) x^T(t) \right] \\
&\quad + 2\lambda l_a^2 e_s(t) e_a(t) \text{tr} \left[ x(t) U^T(t) D(t) D^T(t) C(t) x^T(t) \right] - 2l_a e_a(t) \text{tr} \left[ x(t) C^T(t) D(t) \tilde{w}_a^{(1)}(t) \right] \\
&\quad - 2\lambda l_a e_s(t) \text{tr} \left[ x(t) U^T(t) D(t) \tilde{w}_a^{(1)}(t) \right] \\
&= \text{tr} \left[ \left( \tilde{w}_a^{(1)}(t) \right)^T \tilde{w}_a^{(1)}(t) \right] + l_a^2 e_a^2(t) \|C^T(t) D(t)\|^2 \|x(t)\|^2 + \lambda^2 l_a^2 e_s^2(t) \|U^T(t) D(t)\|^2 \|x(t)\|^2 \\
&\quad + 2\lambda l_a^2 e_s(t) e_a(t) \text{tr} \left[ x(t) U^T(t) D(t) D^T(t) C(t) x^T(t) \right] - 2l_a e_a(t) \text{tr} \left[ x(t) C^T(t) D(t) \tilde{w}_a^{(1)}(t) \right] \\
&\quad - 2\lambda l_a e_s(t) \text{tr} \left[ x(t) U^T(t) D(t) \tilde{w}_a^{(1)}(t) \right]
\end{aligned} \tag{56}$$

Using the cyclic property of the trace  $\text{tr}(ABC) = \text{tr}(BCA)$  and the fact that  $C^T(t) D(t) \tilde{w}_a^{(1)}(t) x(t)$  and  $C^T(t) D(t) \tilde{w}_a^{(1)}(t) x(t)$  are scalars:

$$\begin{aligned}
\text{tr} \left[ x(t) C^T(t) D(t) \tilde{w}_a^{(1)}(t) \right] &= \text{tr} \left[ C^T(t) D(t) \tilde{w}_a^{(1)}(t) x(t) \right] \\
&= C^T(t) D(t) \tilde{w}_a^{(1)}(t) x(t)
\end{aligned} \tag{57}$$

$$\begin{aligned}
\text{tr} \left[ x(t) U^T(t) D(t) \tilde{w}_a^{(1)}(t) \right] &= \text{tr} \left[ U^T(t) D(t) \tilde{w}_a^{(1)}(t) x(t) \right] \\
&= U^T(t) D(t) \tilde{w}_a^{(1)}(t) x(t)
\end{aligned} \tag{58}$$

The cross terms can be transformed using  $-2ab \leq a^2 + b^2$  and Cauchy–Schwarz inequality:

$$\begin{aligned}
-2l_a e_a(t) C^T(t) D(t) \tilde{w}_a^{(1)}(t) x(t) &\leq l_a \left( e_a^2(t) + \|C^T(t) D(t) \tilde{w}_a^{(1)}(t) x(t)\|^2 \right) \\
&\leq l_a \left( e_a^2(t) + \|C^T(t) D(t)\|^2 \|\tilde{w}_a^{(1)}(t) x(t)\|^2 \right)
\end{aligned} \tag{59}$$

$$\begin{aligned}
-2l_a e_s(t) U^T(t) D(t) \tilde{w}_a^{(1)}(t) x(t) &\leq l_a \left( e_s^2(t) + \|U^T(t) D(t) \tilde{w}_a^{(1)}(t) x(t)\|^2 \right) \\
&\leq l_a \left( e_s^2(t) + \|U^T(t) D(t)\|^2 \|\tilde{w}_a^{(1)}(t) x(t)\|^2 \right)
\end{aligned} \tag{60}$$

And

$$\begin{aligned}
\text{tr} \left[ x(t) U^T(t) D(t) D^T(t) C(t) x^T(t) \right] &= \text{tr} \left[ U^T(t) D(t) D^T(t) C(t) x^T(t) x(t) \right] \\
&= \text{tr} \left[ U^T(t) D(t) D^T(t) C(t) \right] \text{tr} \left[ x^T(t) x(t) \right] \\
&= \text{tr} \left[ U^T(t) D(t) D^T(t) C(t) \right] \|x(t)\|^2 \\
&\leq \|U^T(t) D(t)\| \|D^T(t) C(t)\| \|x(t)\|^2 \\
&\leq \|U^T(t) D(t)\| \|C^T(t) D(t)\| \|x(t)\|^2
\end{aligned} \tag{61}$$

which yields

$$\begin{aligned} 2\lambda l_a^2 e_s(t) e_a(t) \text{tr} [x(t) U^T(t) D(t) D^T(t) C(t) x^T(t)] &\leq 2\lambda l_a^2 e_s(t) e_a(t) \|U^T(t) D(t)\| \|C^T(t) D(t)\| \|x(t)\|^2 \\ &\leq l_a^2 (e_a^2(t) \|C^T(t) D(t)\|^2 \|x(t)\|^2 + \lambda^2 e_s^2(t) \|U^T(t) D(t)\|^2 \|x(t)\|^2) \end{aligned} \quad (62)$$

Finally, we can obtain the upper bound

$$\begin{aligned} \Delta L_4(t) &\leq \frac{1}{\gamma_3} \left( 2l_a e_a^2(t) \|C^T(t) D(t)\|^2 \|x(t)\|^2 + e_a^2(t) + \|C^T(t) D(t)\|^2 \left\| \tilde{w}_a^{(1)}(t) x(t) \right\|^2 \right) \\ &+ \frac{\lambda}{\gamma_3} \left( 2\lambda l_a e_s^2(t) \|U^T(t) D(t)\|^2 \|x(t)\|^2 + e_s^2(t) + \|U^T(t) D(t)\|^2 \left\| \tilde{w}_a^{(1)}(t) x(t) \right\|^2 \right) \end{aligned} \quad (63)$$

□

### C. Convergence of the weights errors

We introduce the Lyapunov candidate

$$L(t) = L_1(t) + L_2(t) + L_3(t) + L_4(t) \quad (64)$$

**Theorem 2** (Main Theorem). Let the weights of the critic and actor be updated by gradient descent algorithm, and assume that the one-step cost is a bounded semidefinite function. Under Assumption 1, the estimation errors  $w_c^* - \hat{w}_c(t)$  and  $w_a^* - \hat{w}_a(t)$  are uniformly ultimately bounded (UUB) if

$$l_c < \min_t \frac{\gamma_2 - 1}{\gamma_2 (\|\phi_c(t)\|^2 + \frac{1}{\gamma_2} \|a(t)\|^2 \|y(t)\|^2)} \quad (65)$$

$$l_a < \min_t \frac{\gamma_3 - \gamma_1}{\gamma_3 \|C(t)\|^2 \|\phi_a(t)\|^2 + \gamma_1 \|D(t) C^T\|^2 \|x(t)\|^2} \quad (66)$$

$$l_a < \min_t \frac{1}{2\lambda} \frac{\gamma_3 - \gamma_1}{\gamma_3 \|U(t)\|^2 \|\phi_a(t)\|^2 + \gamma_1 \|U^T(t) D(t)\|^2 \|x(t)\|^2} \quad (67)$$

**Proof of Theorem 2.** Collect all terms of  $\Delta L(t)$  based on the results of Lemmas 1–4,  $\Delta L(t)$  is bounded by

$$\begin{aligned} \Delta L(t) &\leq (\Delta L_1) = l_c \underbrace{e_c^2(t)}_2 \|\phi_c(t)\|^2 + \|e_c(t) - \tilde{w}_c^{(2)}(t) \phi_c(t)\|^2 - \underbrace{\|\zeta_c(t)\|^2}_1 - \underbrace{e_c^2(t)}_2 \\ &+ (\Delta L_2) + \frac{1}{\gamma_1} \left( 2l_a \underbrace{e_a^2(t)}_3 \|C(t)\|^2 \|\phi_a(t)\|^2 + 4\|c(t)\|^2 + 8\alpha^2 \underbrace{\|\zeta_c(t+1)\|^2}_1 + 8\alpha^2 \left\| w_c^{*(2)} \phi_c(t+1) \right\|^2 + \|C(t)\|^2 \|\zeta_a(t)\|^2 - \underbrace{e_a^2(t)}_3 \right) \\ &+ \frac{\lambda}{\gamma_1} \left( 2\lambda l_a \underbrace{e_s^2(t)}_4 \|U(t)\|^2 \|\phi_a(t)\|^2 + 2e_s^2(t) + \|U^T(t) \zeta_a(t)\|^2 - \underbrace{e_s^2(t)}_4 \right) \\ &+ (\Delta L_3) + \frac{1}{\gamma_2} \left( l_c \underbrace{e_c^2(t)}_2 \|a(t)\|^2 \|y(t)\|^2 + \|a(t)\|^2 \|\tilde{w}_c^{(1)}(t) y(t)\|^2 + \underbrace{e_c^2(t)}_2 \right) \\ &+ \Delta L_4(t) + \frac{1}{\gamma_3} \left( 2l_a \underbrace{e_a^2(t)}_3 \|C^T(t) D(t)\|^2 \|x(t)\|^2 + \underbrace{e_a^2(t)}_3 + \|C^T(t) D(t)\|^2 \left\| \tilde{w}_a^{(1)}(t) x(t) \right\|^2 \right) \\ &+ \frac{\lambda}{\gamma_3} \left( 2\lambda l_a \underbrace{e_s^2(t)}_4 \|U^T(t) D(t)\|^2 \|x(t)\|^2 + \underbrace{e_s^2(t)}_4 + \|U^T(t) D(t)\|^2 \left\| \tilde{w}_a^{(1)}(t) x(t) \right\|^2 \right) \end{aligned} \quad (68)$$

Collecting like terms yields

$$\begin{aligned}
\Delta L(t) \leq & - \underbrace{\left( \|\zeta_c(t)\|^2 - \frac{8\alpha^2}{\gamma_1} \|\zeta_c(t+1)\|^2 \right)}_1 - \underbrace{\left( 1 - l_c \|\phi_c(t)\|^2 - \frac{l_c}{\gamma_2} \|a(t)\|^2 \|y(t)\|^2 - \frac{1}{\gamma_2} \right)}_2 e_c^2(t) \\
& - \underbrace{\left( \frac{1}{\gamma_1} - \frac{2l_a}{\gamma_1} \|C(t)\|^2 \|\phi_a(t)\|^2 - \frac{2l_a}{\gamma_3} \|C(t)^T D(t)\|^2 \|x(t)\|^2 - \frac{1}{\gamma_3} \right)}_3 e_a^2(t) \\
& - \underbrace{\left( \frac{\lambda}{\gamma_1} - \frac{2\lambda^2 l_a}{\gamma_1} \|U(t)\|^2 \|\phi_a(t)\|^2 - \frac{2\lambda^2 l_a}{\gamma_3} \|U^T(t) D(t)\|^2 \|x(t)\|^2 - \frac{\lambda}{\gamma_3} \right)}_4 e_s^2(t) \\
& + \|w_c^{*(2)} \phi_c(t) - c(t) - \alpha \hat{w}_c^{(2)}(t) \phi_c(t+1)\|^2 + 4 \|c(t)\|^2 + \frac{8\alpha^2}{\gamma_1} \|w_c^{*(2)} \phi_c(t+1)\|^2 + \frac{1}{\gamma_1} \|C(t)\|^2 \|\zeta_a(t)\|^2 \\
& + 2 \frac{\lambda}{\gamma_1} e_s^2 + \frac{\lambda}{\gamma_1} \|U^T(t) \zeta_a(t)\|^2 + \frac{\lambda}{\gamma_3} \|U^T(t) D(t)\|^2 \|\tilde{w}_a^{(1)} x(t)\|^2 \\
& + \frac{1}{\gamma_2} \|a(t)\|^2 \|\tilde{w}_c^{(1)}(t) y(t)\|^2 \\
& + \frac{1}{\gamma_3} \|C^T(t) D(t)\|^2 \|\tilde{w}_a^{(1)}(t) x(t)\|^2
\end{aligned} \tag{69}$$

**Remark 5.** The bound of  $e_s(t)$  depends on the time step  $T$ , which can be small when using a fast sampling strategy.

To ensure the negativity of the term 1:

$$\frac{\gamma_1}{8\alpha^2} > \frac{\|\zeta_c(t+1)\|^2}{\|\zeta_c(t)\|^2} \tag{70}$$

To find an upper bound of  $\frac{\|\zeta_c(t+1)\|^2}{\|\zeta_c(t)\|^2}$ , we introduce an assumption [30]:

**Assumption 2.** The regressor vector  $\phi(x)$  is persistently exciting and bounded away from zero, which satisfies a non-degeneracy condition such that there exists  $\underline{\kappa} \geq 0$  for which

$$\|\tilde{w}_c^{(2)}(t) \phi(x)\| \geq \underline{\kappa} \|\tilde{w}_c^{(2)}(t)\| \|\phi(x)\|, \forall t \tag{71}$$

Therefore

$$\frac{\|\zeta_c(t+1)\|^2}{\|\zeta_c(t)\|^2} = \frac{\|\tilde{w}_c^{(2)}(t) \phi(x(t+1))\|^2}{\|\tilde{w}_c^{(2)}(t) \phi(x(t))\|^2} \leq \frac{\|\tilde{w}_c^{(2)}(t)\|^2 \|\phi(x+1)\|^2}{\underline{\kappa}^2 \|\tilde{w}_c^{(2)}(t)\|^2 \|\phi(x)\|^2} \leq \frac{\|\phi(x+1)\|^2}{\underline{\kappa}^2 \|\phi(x)\|^2} \leq \frac{N_h}{\underline{\kappa}^2 \phi^2} \tag{72}$$

where  $N_h$  is the upper bound of  $\|\phi(x(t+1))\|^2$ .

Connecting back to (70):

$$\gamma_1 > \frac{8N_h}{\underline{\kappa}^2 \phi^2} \alpha^2 \tag{73}$$

To ensure negativity of the term 2:

$$1 - l_c \|\phi_c(t)\|^2 - \frac{l_c}{\gamma_2} \|a(t)\|^2 \|y(t)\|^2 - \frac{1}{\gamma_2} > 0 \tag{74}$$

Therefore,

$$l_c < \min_t \frac{\gamma_2 - 1}{\gamma_2 (\|\phi_c(t)\|^2 + \frac{1}{\gamma_2} \|a(t)\|^2 \|y(t)\|^2)} \tag{75}$$

In particular,  $\gamma_2 > 1$ .

Similarly, to ensure negativity of the term 3:

$$\frac{1}{\gamma_1} - \frac{2l_a}{\gamma_1} \|C(t)\|^2 \|\phi_a(t)\|^2 - \frac{2l_a}{\gamma_3} \|C^T(t) D(t)\|^2 \|x(t)\|^2 - \frac{1}{\gamma_3} > 0 \tag{76}$$

Therefore,

$$l_a < \min_t \frac{1}{2} \frac{\gamma_3 - \gamma_1}{\gamma_3 \|C(t)\|^2 \|\phi_a(t)\|^2 + \gamma_1 \|C^T(t) D(t)\|^2 \|x(t)\|^2} \tag{77}$$

In particular,  $\gamma_3 > \gamma_1$ .

To ensure negativity of term 4:

$$\frac{\lambda}{\gamma_1} - \frac{2\lambda^2 l_a}{\gamma_1} \|U(t)\|^2 \|\phi_a(t)\|^2 - \frac{2\lambda^2 l_a}{\gamma_3} \|U^T(t)D(t)\|^2 \|x(t)\|^2 - \frac{\lambda}{\gamma_3} > 0 \quad (78)$$

Therefore,

$$l_a < \min_t \frac{1}{2\lambda} \frac{\gamma_3 - \gamma_1}{\gamma_3 \|U(t)\|^2 \|\phi_a(t)\|^2 + \gamma_1 \|U^T(t)D(t)\|^2 \|x(t)\|^2} \quad (79)$$

The fifth term can be bounded as

$$\|w_c^{*(2)}\phi_c(t) - c(t) - \alpha\hat{w}_c^{(2)}(t)\phi_c(t+1)\|^2 \leq 4\|w_c^{*(2)}\phi_c(t)\|^2 + 4c^2(t) + 2\alpha^2\|\hat{w}_c^{(2)}(t)\phi_c(t+1)\|^2 \quad (80)$$

Let  $\bar{C}, \bar{U}, \bar{w}_{a1}, \bar{w}_{a2}, \bar{w}_{c1}, \bar{\phi}_c, \bar{y}, \bar{x}, \bar{a}, \bar{D}, \bar{e}_s$  be upper bounds of  $C, U, \tilde{w}_a^{(1)}, \tilde{w}_a^{(2)}, w_c^{(1)}, \phi_a, \phi_c, y, x, a, D, e_s$ , and let  $\bar{w}_{c2} = \max\{w_c^{*(2)}, \hat{w}_{c2}^{\max}\}$ , where  $\hat{w}_{c2}^{\max}$  is the upper bound of  $\hat{w}_c^{(2)}(t)$ . Finally, we obtain the following bound:

$$\begin{aligned} & \|w_c^{*(2)}\phi_c(t) - c(t) - \alpha\hat{w}_c^{(2)}(t)\phi_c(t+1)\|^2 + 4\|c(t)\|^2 + \frac{8\alpha^2}{\gamma_1}\|w_c^{*(2)}(t)\phi_c(t+1)\|^2 + \frac{1}{\gamma_1}\|C(t)\|^2\|\zeta_a(t)\|^2 \\ & + \frac{1}{\gamma_2}\|a(t)\|^2\|\tilde{w}_c^{(1)}(t)y(t)\|^2 + \frac{1}{\gamma_3}\|C^T(t)D(t)\|^2\|\tilde{w}_a^{(1)}(t)x(t)\|^2 \\ & + 2\frac{\lambda}{\gamma_1}e_s^2 + \frac{\lambda}{\gamma_1}\|U^T(t)\zeta_a(t)\|^2 + \frac{\lambda}{\gamma_3}\|U^T(t)D(t)\|^2\|\tilde{w}_a^{(1)}x(t)\|^2 \\ & \leq \left(\frac{8\alpha^2}{\gamma_1} + 4 + 2\alpha^2\right)(\bar{w}_{c2}\bar{\phi}_c)^2 + 8\bar{c}^2 + \frac{1}{\gamma_1}(\bar{C}\bar{w}_{a2}\bar{\phi}_a)^2 + \frac{1}{\gamma_2}(\bar{w}_{c1}\bar{y}\bar{a})^2 + \frac{1}{\gamma_3}(\bar{C}\bar{D}\bar{w}_{a1}\bar{x})^2 \\ & + 2\frac{\lambda}{\gamma_1}\bar{e}_s^2 + \frac{\lambda}{\gamma_1}(\bar{U}\bar{w}_{a2}\bar{\phi}_a)^2 + \frac{\lambda}{\gamma_3}(\bar{U}\bar{D}\bar{w}_{a1}\bar{x})^2 = M \end{aligned} \quad (81)$$

The conclusion is, if  $\gamma_1 > \frac{8N_h}{\kappa^2\phi^2}\alpha^2$ , and  $l_c, l_a$  satisfying (75), (77), (79) and  $\|\zeta_c(t)\|^2 - \frac{8\alpha^2}{\gamma_1}\|\zeta_c(t+1)\|^2 > M$ , we obtain  $\Delta L(t) < 0$ . This implies that the estimation errors are ultimately uniformly bounded based on Theorem 1.  $\square$

## V. ONLINE LEARNING FLIGHT CONTROL DESIGN

In this section, TS-IHDP is applied to online angle-of-attack tracking control. To address the aerodynamics that degrade control performance, a cascaded control structure is developed using a virtual control approach. This structure explicitly incorporates a pitch-rate reference and is trained via hierarchical reinforcement learning, consisting of outer-loop and inner-loop agents. The switching pitch-rate reference is further passed through a low-pass filter to obtain smooth signals, as is commonly applied in command-filtered backstepping [21], [22].

### A. Angle-of-attack tracking control problem

The dynamical model of aerial vehicles is given as [31]

$$\begin{aligned} \dot{\alpha} &= \left(\frac{fgQS}{WV}\right) \cos(\alpha)[\phi_z(\alpha) + b_z\delta] + q \\ \dot{q} &= \left(\frac{fQSD}{I_{yy}}\right) [\phi_m(\alpha) + b_m\delta] \end{aligned} \quad (82)$$

where  $\alpha$  is the angle of attack,  $q$  is the pitch rate,  $\delta$  is the control surface deflection. The aerodynamic coefficients are seen in Appendix. The tracking errors are defined as  $e_1 = \alpha - \alpha_{\text{ref}}$ ,  $e_2 = q - q_{\text{ref}}$ , where  $\alpha_{\text{ref}}$ ,  $q_{\text{ref}}$  are reference signals, and

$$\begin{aligned} \dot{e}_1 &= \dot{\alpha} - \dot{\alpha}_{\text{ref}} = f_1(\alpha) + e_2 + q_{\text{ref}} + d_1 - \dot{\alpha}_{\text{ref}} \\ \dot{e}_2 &= \dot{q} - \dot{q}_{\text{ref}} = f_2(\alpha) + g_2\delta - \dot{q}_{\text{ref}} \end{aligned} \quad (83)$$

The nonlinear functions are defined as

$$\begin{aligned} f_1(x_1) &= \left(\frac{fgQS}{WV}\right) \cos(\alpha)\phi_z(\alpha), \quad d_1(x_1, u) = \left(\frac{fgQS}{WV}\right) \cos(\alpha)b_z \\ f_2(x_1) &= \left(\frac{fQSD}{I_{yy}}\right) \phi_m(\alpha), \quad g_2(x_1, \delta) = \left(\frac{fQSD}{I_{yy}}\right) b_m \end{aligned} \quad (84)$$

The error dynamics are a single-input-single-output (SISO) system with near-integrator dynamics. When pitch rate control is aggressive, the system exhibits oscillations. Moreover, the aerodynamics  $f_1$  introduce disturbances to both the angle-of-attack tracking error and the control input.

### B. Incremental model

The incremental model of  $q$ -dynamics is

$$\Delta q_{t+1} = F_{t-1} \Delta q_t + G_{t-1} \Delta \delta_t \quad (85)$$

where the subscript  $t$  denotes the discrete-time index. The state increments are defined as  $\Delta q_{t+1} = q_{t+1} - q_t$ ,  $\Delta q_t = q_t - q_{t-1}$ , the control increment is defined as  $\Delta \delta_t = \delta_t - \delta_{t-1}$ . The first-order partial derivatives are  $F_{t-1} = \frac{\partial f_2}{\partial \alpha}|_{\alpha_{t-1}, \delta_{t-1}, q_{t-1}}$ ,  $G_{t-1} = \frac{\partial g_2 u}{\partial \delta_t}|_{\alpha_{t-1}, \delta_{t-1}, q_{t-1}}$ . Only the signs of the control effectiveness  $G_{t-1}$  are needed to construct policy gradients.

### C. Flight control design

1) *Cascaded control structure*: The outer-loop control law and inner-loop control laws are parameterized by  $q_{\text{ref}} = W_1(e_1, \alpha, \delta)$ ,  $\delta = W_2(e_2, q, \alpha)$ . The nested control law is

$$\delta(e_2, q, \alpha) = W_2(q - \underbrace{W_1(e_1, \alpha, \delta)}_{\text{outer-loop actor}}, q, \alpha) \quad (86)$$

$$\underbrace{\quad}_{\text{inner-loop actor}}$$

where  $W_1(\cdot; w^{A_1})$ ,  $W_2(\cdot; w^{A_2})$  are neural networks with trainable parameter sets  $w^{A_1}, w^{A_2}$ . The cascaded actor is illustrated in Figure 1, along with a comparison to the monolithic actor.

2) *Outer-loop agent*: The outer-loop agent learns a pitch rate reference policy based on angle-of-attack tracking performance. Both the critic and actor are fully connected multilayer perceptrons (MLPs). The critic takes  $[\alpha, e_\alpha, q]^T$  as input and outputs the estimated state value  $\hat{V}_1$ . The actor receives  $[\alpha, e_1, \delta]^T$  as input, and its output is pitch rate reference, constrained using a scaled  $\tanh(\cdot)$  function to enforce its limits. The critic is updated via temporal-difference (TD) learning to minimize  $L_t^{C_1} = \frac{1}{2} \delta_{1(t)}^2$ , where  $\delta_{1(t)} = c_{1(t)} + \alpha \hat{V}'_{1(t+1)} - \hat{V}_{1(t)}$  is the TD error,  $\hat{V}'_1(\cdot)$  is the target critic which delays weight updates to stabilize learning.

The one-step cost is

$$c_1(t) = e_1^2(t) + a q_{\text{ref}}^2(t) \quad (87)$$

The multi-objective optimization is formulated as

$$q_{\text{ref}(t)}^* = \arg \min_{v_t} \left( c_{1(t)} + \alpha \hat{V}'_{1(t+1)} + \lambda_1 L_{1(t)}^{\text{TS}} \right) \quad (88)$$

where the temporal smoothness loss

$$L_{1(t)}^{\text{TS}} = |q_{\text{ref}(t+1)} - q_{\text{ref}(t)}| \quad (89)$$

3) *Inner-loop agent*: The inner-loop agent learns a control-surface deflection policy based on the pitch-rate tracking performance. The non-minimum-phase dynamics associated with  $\delta$  may inadvertently affect the  $\alpha$ -dynamics. This motivates the adoption of a cascaded control structure, which isolates this effect from the inner-loop agent's training. As a result, the outer-loop agent is prevented from attempting to control the angle of attack directly using the control-surface deflection.

The critic receives  $[q, e_q]^T$  as input, and outputs the estimated state-value  $\hat{V}_{2(t)}$ . The actor receives  $[q, e_q, \alpha]^T$  as input and outputs the control surface deflection, with scaled  $\tanh(\cdot)$  at the output layer to enforce action limits. The critic is trained to minimize the loss  $L_t^{C_2} = \frac{1}{2} \delta_{2(t)}^2$ , where  $\delta_{2(t)} = c_{2(t)} + \alpha \hat{V}'_{2(t+1)} - \hat{V}_{2(t)}$  is the TD error and  $\hat{V}'_2(\cdot)$  is the target critic, updated as a delayed version of  $\hat{V}_2(\cdot)$  to stabilize learning.

The one-step cost is

$$c_2(t) = e_2^2(t) + b u^2(t) \quad (90)$$

where  $b \in \mathbb{R}_+$  trades off between tracking error and control effort. The optimal control law is defined as

The multi-objective optimization is formulated as

$$\delta_t^* = \arg \min_{\delta_t} \left( c_{2(t)} + \alpha \hat{V}'_{2(t+1)} + \lambda_2 L_{2(t)}^{\text{TS}} \right) \quad (91)$$

where the temporal smoothness loss

$$L_{2(t)}^{\text{TS}} = |\delta_{t+1} - \delta_t| \quad (92)$$

4) *Training*: The action  $q_{\text{ref}}$  is passed through the inner-loop actor to produce the control input  $\delta$ , which directly interacts with the plant model. The inner-loop actor therefore acts as an additional control effectiveness. From the perspective of the outer-loop actor, the plant is effectively an extended system that includes the inner-loop actor (see Figure 1). The outer-loop actor is trained using the transition sample  $(e_{1(t)}, \alpha_t, q_t, \delta_t, q_{\text{ref}}, e_{1(t+1)}, \alpha_{t+1}, q_{t+1})$ , and the inner-loop actor is treated as part of the environment. In contrast, the inner-loop actor is trained independently of the outer-loop actor, since policy gradient propagation does not pass through the outer-loop policy. Its training sample is  $(e_{2(t)}, q_t, \alpha_t, \delta_t, e_{2(t+1)}, q_{t+1})$ . Under this formulation, the environment for inner-loop training consists solely of the  $e_2$ -dynamics.

**Remark 6.** Intuitively, the training of outer-loop actor may require the incremental model of  $\alpha$ -dynamics as it is based on the  $\alpha$  tracking performance. The outer-loop actor still interacts with the model through control surface deflection, i.e. the  $q$ -incremental model, and the  $\alpha$ -incremental model is implicitly contained in  $\hat{V}_2$ .

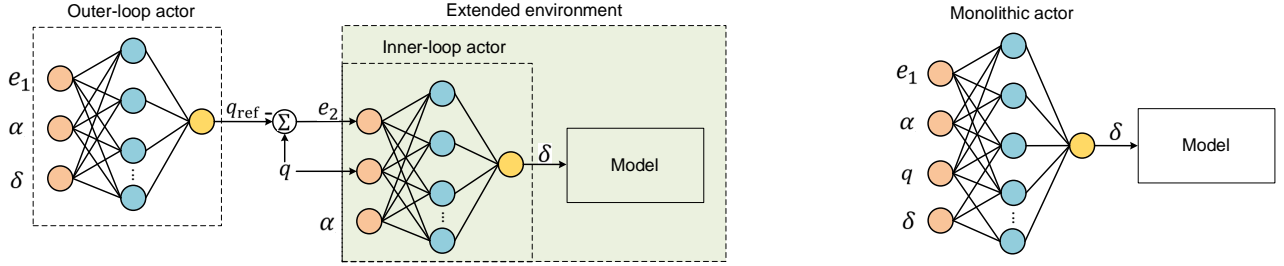


Fig. 1: Cascaded actor versus monolithic actor. The former uses an outer-loop actor to generate a pitch-rate reference, which is then passed to an inner-loop actor that produces the control-surface deflection, providing an explicit mechanism for learning and tracking the pitch-rate reference. The latter is a fully connected multilayer perceptron (MLP) that approximates an end-to-end tracking policy. The pitch-rate reference is not explicitly represented by the monolithic actor. This end-to-end structure is commonly used for the stabilization of inverted pendulum and Van der Pol's oscillator, without additional angular dynamics.

5) *Low-pass filter*: A second-order filter is used to smooth the pitch rate reference:

$$\begin{aligned} \dot{d}_1 &= d_2 \\ \dot{d}_2 &= -2\zeta\omega_n^2 d_2 - \omega_n^2(d_1 - q_{\text{ref}}) \end{aligned} \quad (93)$$

where  $d_1, d_2$  are filtered signal and its differentiation,  $\omega_n$  is the natural frequency,  $\zeta$  is the damping factor.

**Remark 7.** Policy training typically assumes a Markov environment, in which the one-step future state depends only on the current state. However, due to its integral dynamics, the filter state depends on the two previous states, thereby violating the Markov assumption when the filter is included during training of the outer-loop actor. Consequently, gradients from the value function  $\hat{V}_1$  are delayed by two time steps. Although this issue can be addressed by augmenting the environment state with the filter states, doing so increases the computational burden because of the resulting higher system dimensionality. To eliminate gradient delay, this paper excludes the filter from backpropagation of the outer-loop policy gradient and applies it only during forward propagation.

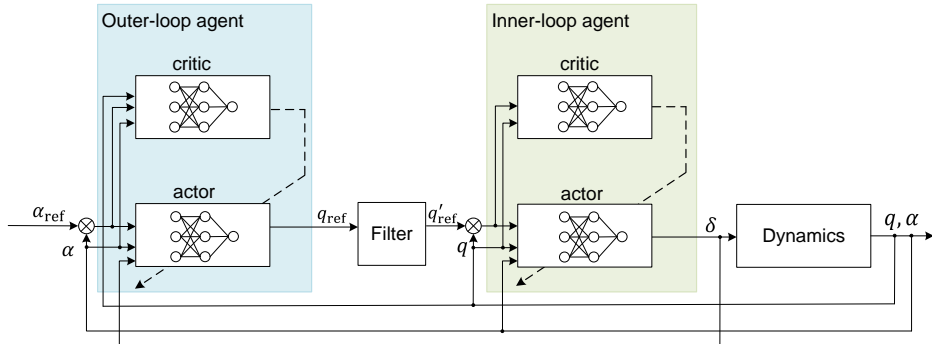


Fig. 2: Command-filtered cascaded online learning flight control system.

## VI. SIMULATION

Simulation results are presented for cascaded online-learning flight control systems. The aerial vehicle dynamics are numerically simulated through the fourth-order Runge Kutta method. The actuator dynamics are modeled as a first-order system  $\tau\dot{\delta}_t + \delta_t = \delta_{c(t)}$ ,  $\tau = 0.005$ . To constrain actions, the outer-loop and inner-loop actors are scaled to  $[-20^\circ, 20^\circ]$  and  $[-20^\circ/\text{s}, 20^\circ/\text{s}]$ . The reference of angle-of-attack is set as  $\alpha_{\text{ref}(t)} = 10^\circ \sin(\frac{2\pi}{T}t)$ ,  $T = 10\text{s}$ . The network weights are randomly initialized using a uniform distribution  $\mathcal{U}(-0.01, 0.01)$ , which ensures an initially low-gain control law and slow learning. This initialization prevents excessive sensitivity to inaccurate policy gradients during the early stages of training. The persistence excitation signal is generated by adding Gaussian noise  $\mathcal{N}(0, 0.04)$  to the control surface deflection. The hyperparameters of the RL agents are listed in Table I. The baseline control system operates without a filter and employs IHDP, i.e.  $\lambda_{1,2} = 0$ . We discuss the performance in terms of tracking control, action smoothness, activation function saturation, action increments, and actor sensitivity.

TABLE I: Hyperparameters of RL agents

Parameter	Outer-loop agent	Inner-loop agent
critic learning rate $l_{c1}, l_{c2}$	0.1	0.1
actor learning rate $l_{a1}, l_{a2}$	$5 \times 10^{-7}$	$10^{-7}$
discount factor $\alpha$	0.6	0.6
delay factor $\tau$	1	1
hidden layer size	7	7
critic hidden-layer activation function	tanh	tanh
actor activation function	tanh	tanh
control effort weights $a, b$	$5 \times 10^{-6}$	$10^{-5}$
smoothness loss weight $\lambda_1, \lambda_2$	$9.3 \times 10^{-4}$	$10^{-5}$

### A. Tracking performance and control smoothness

1) *Tracking control:* In Figure 3, IHDP-based control system learns tracking the angle-of-attack reference during the first 10 seconds, then experiences growing oscillations with increasing tracking errors after 32s. The outer-loop and inner-loop actors are near-saturated after 32s and 23s, respectively. The amplitude of action oscillation is reduced by using a hard action constraint within  $\pm 5^\circ$  in [9], but the policy becomes a bang-bang control with constrained amplitude. In contrast, TS-IHDP learns an action-increment-constrained policy, naturally generating actions within  $\pm 6^\circ$ , and prevents actor saturation as shown in Figure 7. In Figure 4, the critic weights converge to sub-optimal values within 10s. Oscillations happen after 30s in IHDP-based control system. The actor weights of TS-IHDP-based control system grow slightly more slowly due to the stabilized tracking errors.

**Challenges on TS-IHDP-based control system.** Control smoothness of TS-IHDP is sensitive to the empirical tuning of  $\lambda_1, \lambda_2$ . Large values reduce exploration of the state space, whereas small values degrade control smoothness. Moreover, TS-IHDP-based control system still exhibits frequently switching actions when tracking errors are near zero. This is because small action increments are only lightly penalized by the temporal smoothness loss (see Equations 89, 92). The frequently switching pitch rate reference further induces switching control surface deflections with amplified amplitudes through the inner-loop actor.

Therefore, we introduce a low-pass filter into the cascaded control system. The natural frequency and damping ratio are  $\omega_n = 20\text{rad/s}$  and  $\zeta = 0.7$ . The comparison between TS-IHDP and command-filtered TS-IHDP shows the filter generates a smoother pitch rate reference and further leads to smoother control surface deflection.

2) *Control smoothness:* Control smoothness is evaluated in the frequency domain using the Fast Fourier Transform (FFT), which transforms the action sequence from the time domain to the frequency domain, as defined by the Discrete Fourier Transform  $X[k] = \sum_{n=0}^{N-1} x[n] e^{-j \frac{2\pi}{N} kn}$ ,  $k = 0, 1, \dots, N-1$ . The spectra in Figures 5 and 6 show that the components of  $q_{\text{ref}}$  below 100 Hz are attenuated by TS-IHDP, and the signal amplitudes are significantly reduced without compromising tracking performance. Similar results are observed for control surface deflection. The switching control surface deflection is a result of the forward propagation of the switching tracking error  $e_2$  through the inner-loop actor. For command-filtered TS-IHDP, these action signals in the 10-40Hz range are effectively attenuated by the filter.

3) *Activation function:* The activation function  $\tanh(\cdot)$  outputs values near its maximum or minimum, and its derivative vanishes when the inputs are large (see Figure 7). Consequently, policy learning becomes slow due to vanishing policy gradients. Another issue is the bang-bang control behavior of a saturated actor in response to small tracking errors, which degrades tracking performance and system stability.

Actor saturation results from an aggressive policy learning process, which occurs for two main reasons: (1) large learning rates. A large learning rate causes the actor weights to be updated with large increments, pushing the activation functions into their saturation regions. This process is effectively irreversible due to vanishing gradients. (2) Underemphasized control effort in the one-step cost function. A one-step cost function that underemphasizes control effort encourages the use of large actions during learning. As a result, the aggressive policy persists and continues to degrade tracking performance even as the tracking error decreases, due to vanishing policy gradients. During 10–20 s, switching actions occur even though  $\tanh(\cdot)$  is

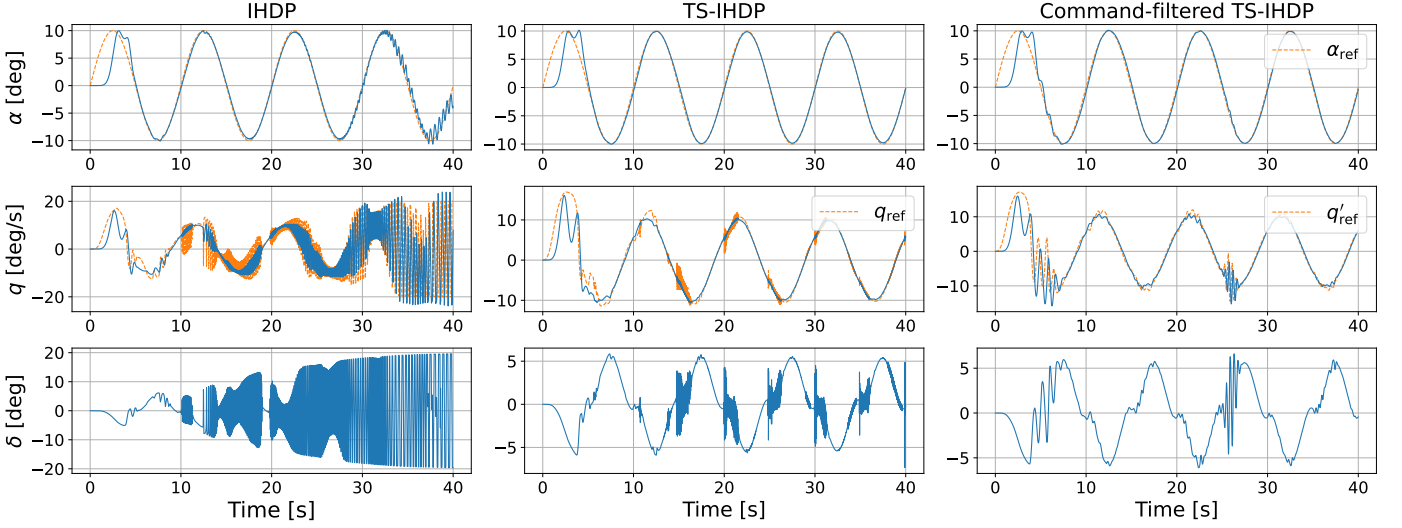


Fig. 3: Tracking control performance.

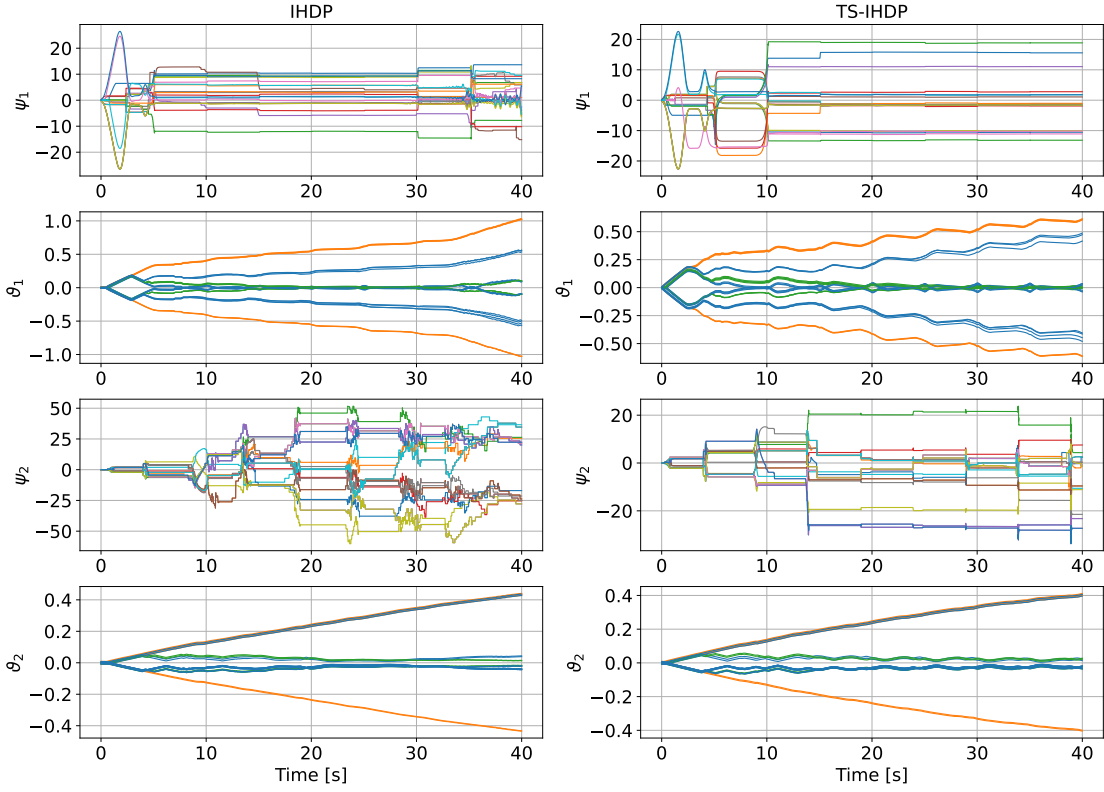


Fig. 4: Critic and actor parameters.

not saturated, indicating that an unsaturated actor can also generate oscillatory actions. Moreover, the time-varying dynamics and time-varying signal  $\alpha_{\text{ref}}$  cause switching tracking error  $e_1$ , which propagate through the outer-loop actor and inner-loop actor to generated switching pitch-rate reference and switching control surface deflections. The pitch-rate reference exhibits switching control without saturation, indicating that the actor does not need to reach saturation to display bang–bang control behavior.

In Figure 7, IHDP makes the inputs of  $\tanh(\cdot)$  within intervals  $[-4, -2]$ ,  $[2, 4]$  (the outer-loop actor) and intervals  $[-3, -2]$ ,  $[2, 3]$  (the lower-level actor). In these intervals, the derivative satisfied  $\tanh'(\cdot) \leq 0.1$  and attenuates the overall policy gradient. As a comparison, TS-IHDP and command-filtered TS-IHDP prevent reaching to the saturation regions. The inputs are kept within ‘unsaturated’ intervals  $[-2, 2]$  (the outer-loop actor) and  $[-0.5, 0.5]$  (the inner-loop actor). The derivative satisfies  $\tanh'(\cdot) \geq 0.4$  (the outer-loop actor) and  $\tanh'(\cdot) \geq 0.8$  (the inner-loop actor). This demonstrates the effectiveness of TS losses in mitigating actor saturation, as the saturated actor generates large action increments.

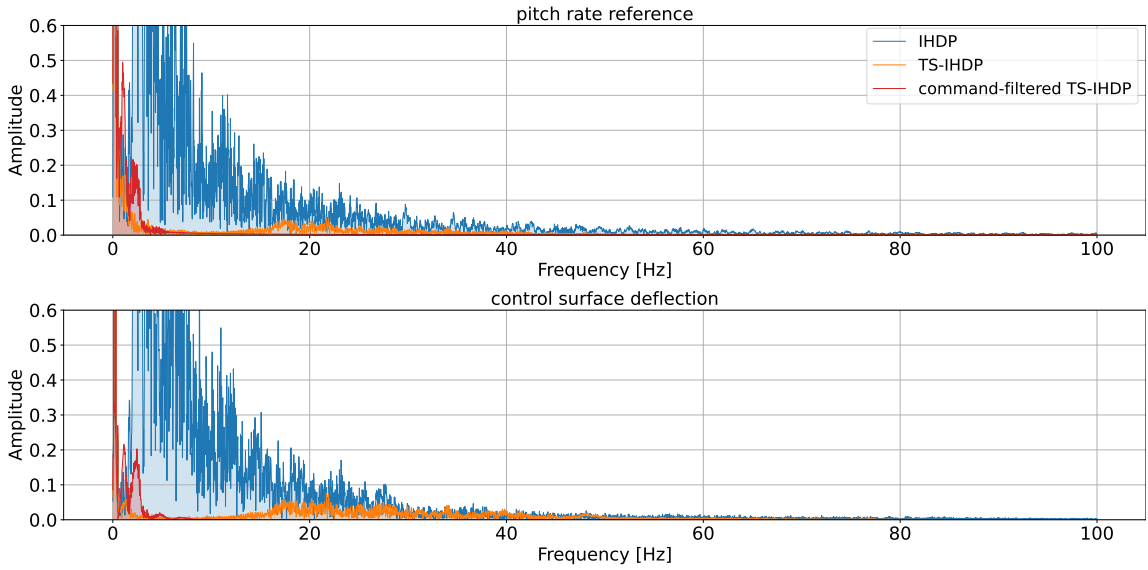


Fig. 5: Spectrum of actions.

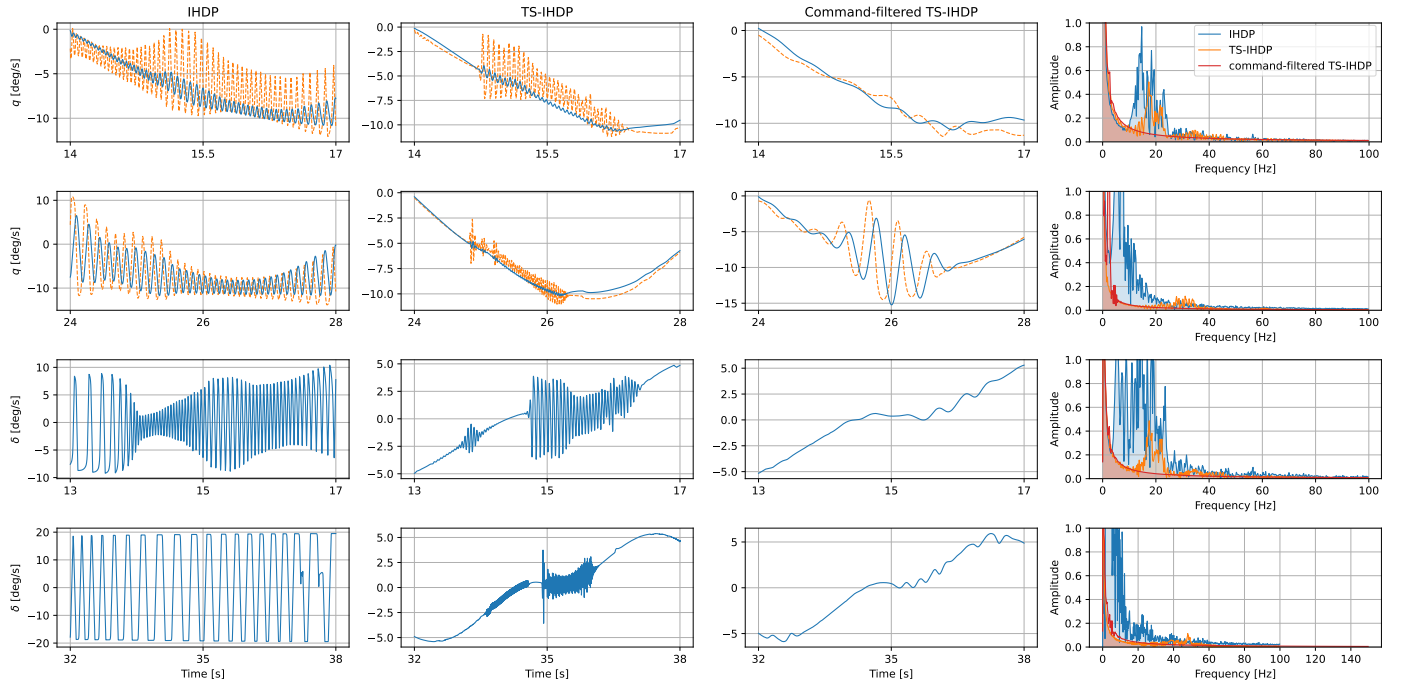


Fig. 6: Action smoothness in selected time intervals.

4) *Action increment*: The one-step action increments are  $\Delta q_{ref(t+1)} = |q_{ref(t+1)} - q_{ref(t)}|$ ,  $\Delta \delta_{t+1} = |\delta_{t+1} - \delta_t|$ . Figure 8 shows the IHDP exhibits large-amplitude and fast-switching action increments, while TS-IHDP reduces the action increment to  $|\Delta q_{ref(t+1)}| \leq 0.5 \text{ } ^\circ/\text{s}$  and reduces the amplitude of  $|\Delta \delta_{t+1}|$ .

5) *Actor sensitivity*: The actor sensitivity indicates how much, and in what direction, the output changes when the input increases slightly. The sensitivity measures of the outer-loop and inner-loop actors are

$$\begin{aligned} K_{1(t)} &= \frac{\partial q_{ref(t)}}{\partial e_{1(t)}} \\ K_{2(t)} &= \frac{\partial \delta(t)}{\partial e_{2(t)}} \end{aligned} \quad (94)$$

The relation between the pitch rate reference and its sensitivity measure is

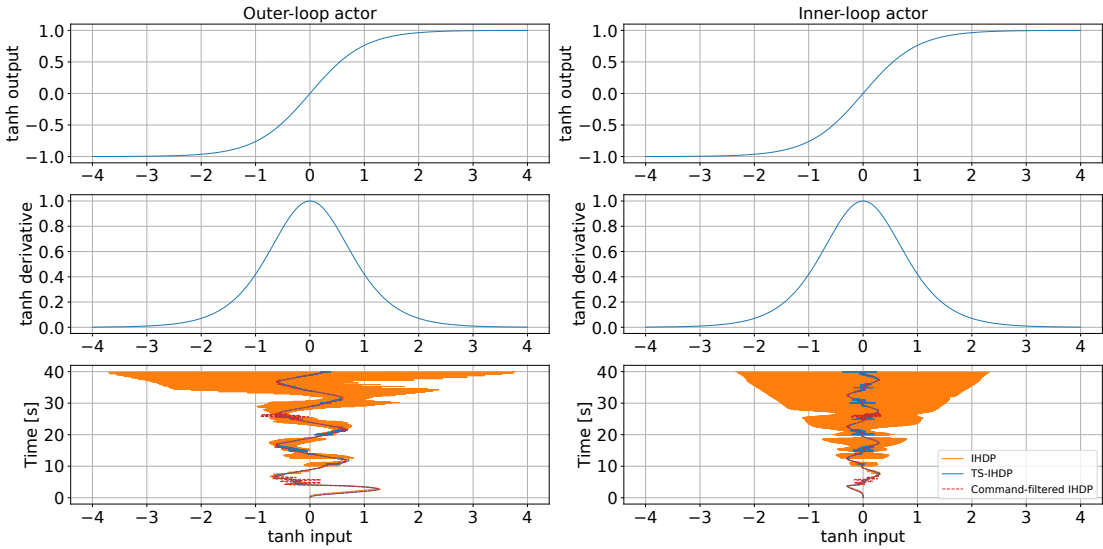
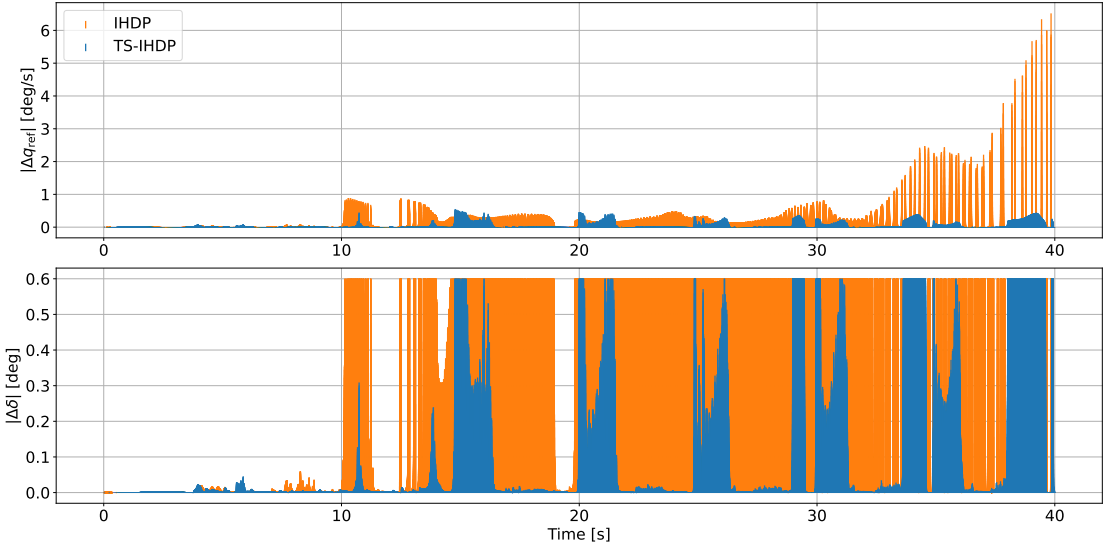
Fig. 7:  $\tanh(\cdot)$  in output layers of actors.

Fig. 8: Increments of actions.

$$\begin{aligned}
 & |q_{\text{ref}(t+1)} - q_{\text{ref}(t)}| \\
 & \approx |K_{1(t)}(e_{1(t+1)} - e_{1(t)})| \\
 & = |K_{1(t)}| \cdot |e_{1(t+1)} - e_{1(t)}|
 \end{aligned} \tag{95}$$

Similarly,

$$\begin{aligned}
 & |\delta_{t+1} - \delta_t| \\
 & \approx |K_{2(t)}(e_{2(t+1)} - e_{2(t)})| \\
 & = |K_{2(t)}| \cdot |e_{2(t+1)} - e_{2(t)}|
 \end{aligned} \tag{96}$$

Therefore, the actor sensitivity can be reduced through constraining action increments. In Figure 9, the comparisons on  $K_1, K_2$  show that applying a filter slows their growth and reduces high-frequency switches, contributing to a more robust controller.

### B. Terminate and restart learning

1) *Termination*: The previous analysis assumes continual learning; that is, the agents never terminate learning during system operation. The issue lies in that growing control gains can cause state oscillations, even when tracking errors are small. Therefore,

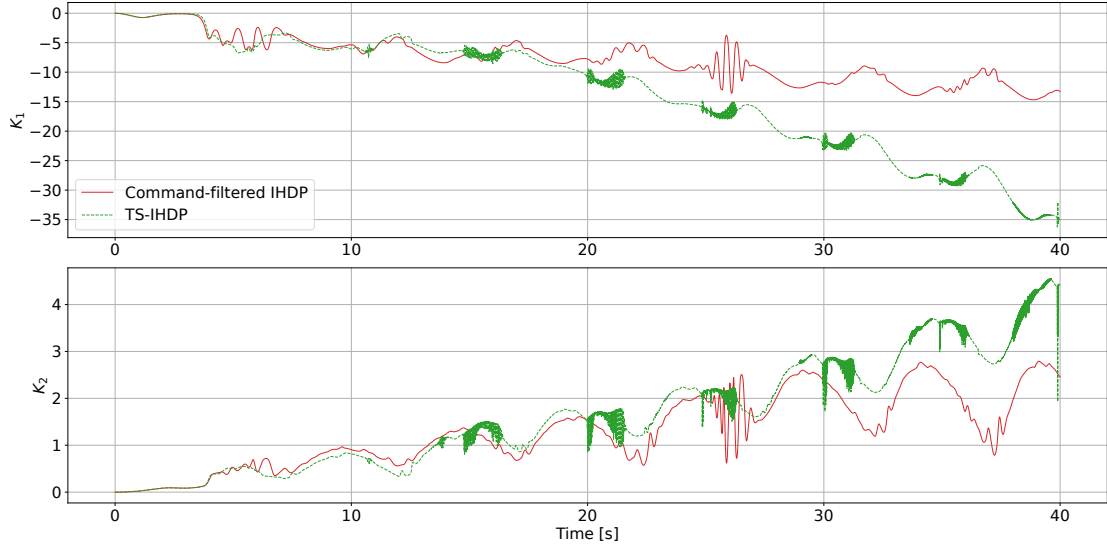


Fig. 9: Sensitivity measures.

it is intuitive to terminate learning when the required tracking performance is satisfied. Specifically, the actor weights are fixed if the accumulated tracking error over a period  $T_s$  remains within a specified threshold:

$$\bar{e}_s \leq \epsilon \quad (97)$$

where  $\bar{e}_s = \frac{1}{n_s} \sum_{i=0}^{n_s-1} |e_{t-i}|$  is the average of absolute tracking errors,  $n_s = T_s / \Delta T$  is the number of samples,  $\epsilon > 0$  is an error threshold. A large  $\epsilon$  makes learning terminated early when tracking performance is unsatisfactory. Define the online-learning state indicator as  $\tau \in \{1, 0\}$ , with  $\tau = 1$  denoting that learning is off and  $\tau = 0$  denoting that learning is on.

During the initial phase, when  $t < T_s$  and there are not enough samples to compute  $\bar{e}_s$ , learning remains active:

$$\tau = 0, \text{ if } t < T_s \quad (98)$$

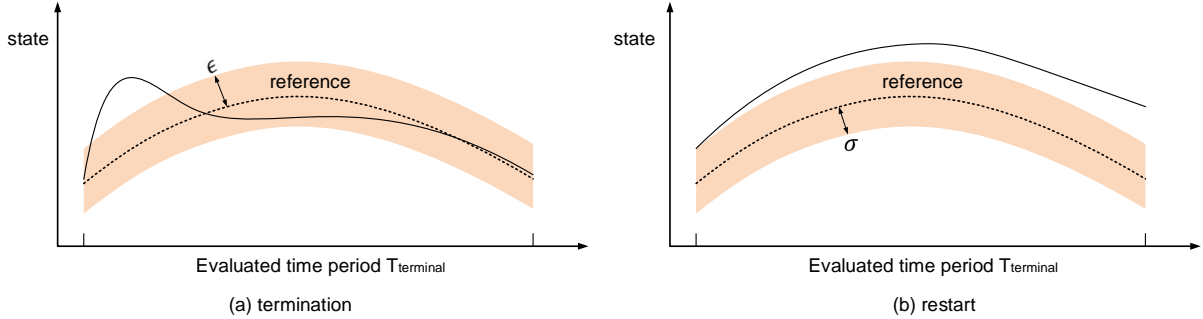


Fig. 10: Termination case (left) and restart case (right). The shaded area represents a performance threshold. The actual average tracking errors must remain below this threshold to terminate learning, and exceed it to trigger a restart.

2) *Restart*: The learning must restart when the historical control performance degrades, typically occurring when the control system falls into faults and uncertainties. The restart condition determines in what case to restart learning. The evaluation period, denoted by  $T_r$ , should be carefully chosen to ensure it qualifies to represent the required control performance. A long evaluation period would delay the restart, preventing a timely response to performance degradation, while a short evaluation period makes the restart decision overly sensitive, potentially triggered by measurement noise or short-term peaks of tracking errors. As a result, the learning state may switch frequently between on and off.

The restart condition is

$$\bar{e}_r \geq \sigma \quad (99)$$

where  $\bar{e}_r = \frac{1}{n_r} \sum_{i=0}^{n_r-1} |e_{t-i}|$  is the averaged absolute tracking errors,  $n_r = T_r/\Delta T$  is the number of samples,  $\sigma > 0$  is an error threshold. The sketch maps are provided in Figure 10. The pseudocode is seen in Algorithm 1.

The outer-loop and inner-loop agents have independent termination and restart conditions. Their parameters are seen in Table II. Figure 11 shows the histories of average tracking errors and the indicators. The outer-loop agent is turned off at 29s and restarted at 31.5s, while the inner-loop agent is turned off at 22s and is never restarted.

**Algorithm 1:** Termination and restart algorithm

---

**Data:**  $T_s, \epsilon, T_r, \sigma, t, \Delta T$

**1 Initialization** termination indicator  $\tau_{t-1} = 0$

**2 for** each environment step  $t \leftarrow t$  to  $t_{\max}$  **do**

**3 if**  $\tau_{t-1} = 0$  **then**

**4 if**  $t \leq T_s$  **then**

**5**  $\tau_t = 0$

**else**

**7 if**  $\bar{e}_s \leq \epsilon$  **then**

**8**  $\tau_t = 1$

**9 else**

**10**  $\tau_t = 0$

**11 end**

**end**

**13 end**

**14 end**

**15 if**  $\tau_{t-1} = 1$  **then**

**16 if**  $\bar{e}_r \geq \sigma$  **then**

**17**  $\tau_t = 0$

**else**

**19**  $\tau_t = 1$

**end**

**21 end**

---

TABLE II: Parameters

Parameter	Outer-loop agent	Inner-loop agent
$T_s$	10s	10s
$\epsilon$	0.25°	0.5deg/s
$T_r$	0.2s	0.1s
$\sigma$	0.8°	2deg/s

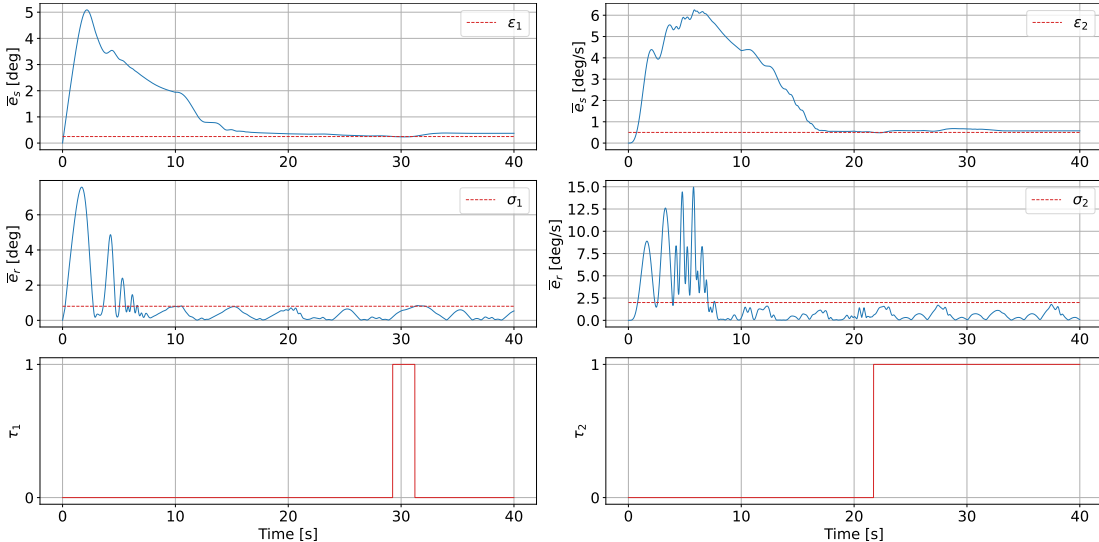


Fig. 11: Termination and restart measures.

## VII. CONCLUSION

We studied temporally smoothed incremental heuristic dynamic programming (TS-IHDP) for online learning. Trace analysis shows that the critic and actor weights converge to suboptimal values in the sense of ultimate uniform boundedness (UUB), where the actor is updated using an additional temporal smoothness loss. Flight control simulations verify the effectiveness of TS-IHDP in learning an action-increment-constrained policy, thereby avoiding actor saturation and degraded tracking performance. The low-pass filter is shown to effectively remove high-frequency components of the pitch-rate reference, which cannot be achieved by TS-IHDP alone. The combination of these two methods enables a sufficient level of action smoothness during online learning. These techniques are essential for online learning-based tracking control of aerial vehicle systems with time-varying dynamics, which are prone to state and action oscillations caused by switching tracking errors. The termination and restart conditions allow the learning process to be autonomously activated and deactivated.

## REFERENCES

- [1] R. Konatala, R. Müller, M. May, G. Looye and E. van Kampen Verification & Validation (V&V) of Reinforcement Learning based Online Adaptive Flight Control Laws on CS-25 Class Aircraft *Euro GNC*, 2024, doi: 10.82124/CEAS-GNC-2024-062.
- [2] R. Konatala, D. Milz, C. Weiser, G. Looye and E. van Kampen Flight Testing Reinforcement-Learning-Based Online Adaptive Flight Control Laws on CS-25-Class Aircraft *Journal of Guidance, Control and Dynamics*, vol. 47, no. 11, pp. 2460–2467, 2024, doi: 10.2514/1.G008321.
- [3] Y. Zhou, E. van Kampen and Q.P. Chu Incremental Model Based Online Dual Heuristic Programming for Nonlinear Adaptive Control *Control Engineering Practice*, vol. 73, pp. 13–25, 2018, doi: 10.1016/j.conengprac.2017.12.011.
- [4] Y. Zhou, E. van Kampen and Q. P. Chu Incremental Approximate Dynamic Programming for Nonlinear Flight Control Design In *Proceedings of the EuroGNC 2015*, Toulouse, France, 2015.
- [5] Y. Zhou, E. van Kampen and Q. P. Chu Incremental Approximate Dynamic Programming for Nonlinear Adaptive Tracking Control with Partial Observability *Journal of Guidance, Control, and Dynamics*, vol. 41, no. 12, pp. 2554–2567, 2018, doi: 10.2514/1.G003472.
- [6] Y. Zhou, E. van Kampen and Q.P. Chu An Incremental Approximate Dynamic Programming Flight Controller Based on Output Feedback *AIAA Guidance, Navigation, and Control Conference*, San Diego, California, USA, January, 2016, doi: 10.2514/6.2016-0360.
- [7] B. Sun and E. van Kampen Incremental Model-Based Global Dual Heuristic Programming with Explicit Analytical Calculations Applied to Flight Control *Engineering Applications of Artificial Intelligence*, vol. 89, pp. 103425, 2020, doi: 10.1016/j.engappai.2019.103425.
- [8] B. Sun and E. van Kampen Intelligent Adaptive Optimal Control Using Incremental Model-Based Global Dual Heuristic Programming Subject to Partial Observability *Applied Soft Computing*, vol. 103, pp. 1–15, 2021, doi: 10.1016/j.asoc.2021.107153.
- [9] B. Sun and E. van Kampen Reinforcement-Learning-Based Adaptive Optimal Flight Control with Output Feedback and Input Constraints *Journal of Guidance, Control, and Dynamics*, vol. 44, no. 9, pp. 1685–1691, 2021, doi: 10.2514/1.G005715.
- [10] B. Sun and E. van Kampen Event-Triggered Constrained Control Using Explainable Global Dual Heuristic Programming for Nonlinear Discrete-Time Systems *Neurocomputing*, vol. 468, pp. 452–463, 2022, doi: 10.1016/j.neucom.2021.10.046.
- [11] Y. Zhou, E. van Kampen and Q.P. Chu Incremental Model Based Heuristic Dynamic Programming for Nonlinear Adaptive Flight Control In *Proceedings of the International Micro Air Vehicles Conference and Competition*, Beijing, China, October, 2016, url: <https://www.imavs.org/papers/2016/25.pdf>.
- [12] Y. Zhou, E. van Kampen and Q. P. Chu Incremental Model based Online Heuristic Dynamic Programming for Nonlinear Adaptive Tracking Control with Partial Observability *Aerospace Science and Technology*, vol. 105, pp. 1–14, 2020, doi: 10.1016/j.ast.2020.106013.
- [13] S. Heyer, D. Kroeseen and E. van Kampen Online Adaptive Incremental Reinforcement Learning Flight Control for a CS-25 Class Aircraft *AIAA Scitech 2020 Forum*, Orlando, FL, USA, October, 2020, doi: 10.2514/6.2020-1844.
- [14] L.G. Sun, C.C. de Visser, Q.P. Chu and W. Falkena Hybrid Sensor-Based Backstepping Control Approach with Its Application to Fault-Tolerant Flight Control *Journal of Guidance, Control, and Dynamics*, vol. 31, no. 1, pp. 59–71, 2014, doi: 10.2514/1.61890.
- [15] Y. Zhou, E. van Kampen and Q.P. Chu Launch Vehicle Adaptive Flight Control with Incremental Model Based Heuristic Dynamic Programming *International Astronautical Congress*, Adelaide, Australia, September, 2017.
- [16] K. G. Vamvoudakis and F. L. Lewis Online actor-critic algorithm to solve the continuous-time infinite horizon optimal control problem *Automatica*, vol. 46, no. 5, pp. 878–888, 2010, doi: 10.1016/j.automatica.2010.02.018.
- [17] F. L. Lewis, D. Vrabie, and V. L. Syrmos *Optimal Control, 3rd edition*. Wiley, Hoboken, NJ, USA, 2009.
- [18] S. Sieberling, Q. P. Chu, and J. A. Mulder Robust Flight Control Using Incremental Nonlinear Dynamic Inversion and Angular Acceleration Prediction *Journal of Guidance, Control and Dynamics*, vol. 33, no. 6, pp. 1732–1742, 2010, doi: 10.2514/1.49978.
- [19] Yury Sokolov, Robert Kozma, Ludmilla D. Werbos, Paul J. Werbos *Automatica*, vol. 59, pp. 9–18, 2015, doi: 10.1016/j.automatica.2015.06.001.
- [20] F. Liu, J. Sun, J. Si, W. Guo and S. Mei *Neural Networks*, vol. 32, pp. 229–235, 2012, doi: 10.1016/j.neunet.2012.02.005.
- [21] A.N. Kalliny, A.A. El-Badawy and S.M. Elkhamisy Command-Filtered Integral Backstepping Control of Longitudinal Flapping-Wing Flight *Journal of Guidance, Control, and Dynamics*, vol. 41, no. 7, pp. 1556–1568, 2018, doi: 10.2514/1.G003267.
- [22] J.A. Farrell, M. Polycarpou, M. Sharma and W. Dong Command Filtered Backstepping *IEEE Transactions on Automatic Control*, vol. 54, no. 6, pp. 1391–1395, 2009, doi: 10.1109/TAC.2009.2015562.
- [23] Q. Wei, Z. Niu, B. Chen, and X. Huang Bang-bang control applied in airfoil roll control with plasma actuators *Journal of Aircraft*, vol. 50, no. 2, pp. 670–677, 2013, doi: 10.2514/1.C031964.
- [24] S. Mysore, B. Mabsout, R. Mancuso and K. Saenko Regularizing Action Policies for Smooth Control with Reinforcement Learning *IEEE International Conference on Robotics and Automation*, Xi'an, China, October, 2021, doi: 10.1109/ICRA48506.2021.9561138.
- [25] V. Gavra, E. van Kampen, Evolutionary reinforcement learning: hybrid approach for safety-informed fault-tolerant flight control, *Journal of Guidance, Control and Dynamics*, vol.47, no.5, pp. 887-900, 2024, doi: 10.2514/1.G008112.
- [26] K. Dally, E. van Kampen, Soft actor-critic deep reinforcement learning for fault tolerant flight control, *AIAA Scitech 2022 Forum*, San Diego, CA & Virtual, USA, 2020, doi: 10.2514/6.2022-2078.
- [27] L. Vieira dos Santos and E. van Kampen, Safe & smart control: hybrid and distributional reinforcement learning for attitude flight control, *AIAA Scitech 2025 Forum*, Orlando, FL, USA, 2025, doi: 10.2514/6.2022-2078.
- [28] M. Homola, E. van Kampen, Uncertainty-driven distributional reinforcement learning for flight control, *AIAA Scitech 2025 Forum*, Orlando, FL, USA, 2025, doi: 10.2514/6.2025-2793.
- [29] A. Niederlinski, An upper bound for the recursive least squares estimation error, *IEEE Transactions on Automatic Control*, vol.40, no.9, pp. 1655-1660, 1995, doi: 10.1109/9.412640.
- [30] Benjamin M. Jenkins, Anuradha M. Annaswamy, Eugene Lavretsky, and Travis E. Gibson Convergence Properties of Adaptive Systems and the Definition of Exponential Stability *SIAM Journal of Control and Optimization*, vol. 56, no. 4, pp. 2463–2484, 2018, doi: 10.1137/15M1047805.
- [31] R.A. Hull, D. Schumacher and Z.H. Qu Design and Evaluation of Robust Nonlinear Missile Autopilots from a Performance Perspective In *Proceedings of 1995 American Control Conference*, Seattle, WA, USA, June, 1995, doi: 10.1109/ACC.1995.529235.

## APPENDIX

## A. Aerodynamic coefficients

The aerodynamic coefficients are approximately computed by  $b_z = -0.034$ ,  $b_m = -0.206$ , and

$$\begin{aligned}\phi_z(\alpha) &= 0.000103\alpha^3 - 0.00945\alpha|\alpha| - 0.170\alpha \\ \phi_m(\alpha) &= 0.000215\alpha^3 - 0.0195\alpha|\alpha| - 0.051\alpha\end{aligned}\quad (100)$$

These approximations of  $b_z, b_m, \phi_z(\alpha), \phi_m(\alpha)$  hold for  $\alpha$  in the range of  $\pm 20$  degrees. The physical coefficients are provided in Table III. In addition, the actuator dynamics are considered as a first order model with the time constant 0.005s. The rate limit is 600 deg/s, and a control surface deflection limit is  $\pm 20$  degrees.

TABLE III: Physical parameters (adapted from [31])

Notations	Definition	Value
$g$	acceleration of gravity	9.815 m/s <sup>2</sup>
$W$	weight	204.3 kg
$V$	speed	947.715 m/s
$I_{yy}$	pitch moment of inertia	247.438 kg· m <sup>2</sup>
$f$	radians to degrees	$180/\pi$
$Q$	dynamic pressure	29969.861 kg/m <sup>2</sup>
$S$	reference area	0.041 m <sup>2</sup>
$d$	reference diameter	0.229 m